The Thesis committee for African University of Science and Technology certifies that this is the approved version of the following thesis:

VERTICAL-HORIZONTAL PERMEABILITY RELATIONSHIPS IN STRESS AND NON-STRESS SENSITIVE RESERVOIRS

APPROVED BY

SUPERVISING COMMITTEE:

Supervisor: _____
Djebbar Tiab

Committee : _____
Samuel Osisanya

_____
Alpheus Ighokoyi

Chief Academic Officer: _____
Godwin Chukwu

December 2011

Major Subject: Petroleum Engineering

VERTICAL-HORIZONTAL PERMEABILITY RELATIONSHIPS IN STRESS AND NON-STRESS SENSITIVE RESERVOIRS

A Thesis

By

PHILIP CHIDIEBERE IHEANACHO

Submitted to the Office of Graduate Studies of

African University of Science and Technology

In partial fulfillment of the requirements for the degree of

MASTER OF SCIENCE

African University of Science and Technology

December 2011

Major Subject: Petroleum Engineering

DEDICATION

I dedicate this work to both of my fathers and all those who have lovingly supported me throughout life and all its travails.

ACKNOWLEDGEMENT

First, I want to give praises to Almighty God for sparing my life, continuously granting me His blessings and allowing me successfully concluding this phase of my life. I also want to acknowledge my supervisor, Dr. Djebbar Tiab for being a mentor and a friend and for always responding promptly to all my e-mails no matter the time of the day. I am honored to have worked with him. I want to acknowledge the supports and contributions of my committee members, Dr. Samuel Osisanya , and Dr. Alpheus Igbokoyi, whose classes are among my favorites and invaluable, and Dr. and Dr. Mrs. Godwin Chukwu for their parental advises guidance and support throughout my stay in the African University of Science and Technology.

I want to acknowledge the eternal support of my mum, Blessed Elizabeth Iheanacho, and my siblings- Dominic, Ifeanyichukwu, Emmanuel, Okwudili, Ada, Okechukwu, and Chinyere- and to my lovely betrothed, Ifeyinwa Chikezie.

ABSTRACT

One of the important petrophysical parameter in reservoir description is the permeability distribution in a given reservoir. It is well known that most reservoir are heterogeneous in nature and homogeneous ones been the few exceptions. Therefore, most reservoirs exist with different degree of permeability anisotropy and reservoir heterogeneity.

In stress sensitive reservoirs, permeability does not only vary spatially but also varies temporally due to the changes in effective stress distribution resulting from pressure drawdown around a producing well and the reservoir pressure distribution due to production and injection processes.

This work investigates the relationship between vertical and horizontal permeability in stress and non-stress sensitive reservoirs. Various petrophysical properties were calculated from core and log data gotten from both stress and non-stress sensitive formations. New correlations between vertical and horizontal permeability were then developed for the zones that were analyzed, with each zone representing different formation types.

The correlations show that there is a log-log linear relationship between vertical and horizontal permeability for the different zones and that these correlations are affected by the shaliness of each zone, and the number of flow units in each zone.

TABLE OF CONTENTS

LIST OF FIGURES

FIGURE Page

CHAPTER ONE

INTRODUCTION

1.1 Problem Description

Stress sensitive reservoirs are reservoirs that their petrophysical properties changes as the stress state of the reservoir changes. This can be seen as a change in matrix pore throat or a change in the apertures of natural fractures. During production and or injection, the reservoir pore pressure changes. This change in pore pressure causes the effective stress of the reservoir to change which leads to a changing stress state. As the stress state of the reservoir changes, different rock properties of the reservoir changes base on the effective stress laws that control each of the petrophysical property.

The presence of clay minerals in stress sensitive formation also affects rock properties of such formation. The clay type, volume fraction and morphology play an important role in controlling the formation properties.

In building a reservoir model for reservoir simulation of stress sensitive formation, the geomechanical and fluid flow properties have to be coupled to capture the effect of the changes in the reservoir stress state. The effect of stress sensitivity is more common to tight, over-pressured and naturally fractured formation.

1.2 Objective

The main objective of this work is to develop different correlations between the vertical permeability and the horizontal permeability for different stress and non-stress sensitivity formations with different formation characteristics. Log and core data from different fields are gathered and analyzed. Some formation properties like effective porosity and shale fraction are taken from the data and their effects on permeability anisotropy (vertical to horizontal permeability) are considered. Different parameters are plotted to show their correlation coefficient and the reliability of such correlation. The developed relationships and their analytical implications are discussed.

1.3 Methodology

A sandstone, limestone and dolostone formations were used for this study. Log and core data taken from three different fields were analyzed. These fields are in Nigeria, Iran and Saudi Arabia. Different parameters like horizontal and vertical permeability measurements, shale volume fraction, and effective porosity were extracted from the data. These parameters were then plotted against each other to generate different correlations. From each correlation, generalized vertical permeability relationships, with good correlation coefficient, were developed for different formation type.

1.4 Organization of This Thesis

The study is divided into five chapters. The outline and organization of this work are as follows:

Chapter I presents an overview of stress sensitive formation. The research problem is described and the project objective is presented.

Chapter II pres**e**nts an extensive literature review. The effects of effective stress on petrophysical properties of formations are reviewed. Different methods used to analyze stress sensitive formations are also reviewed.

Chapter III explains the underlying theory of permeability relationships

Chapter IV describes the sample field cases used in the analysis.

Chapter V presents the results and discussions of the different field cases.

Chapter VI presents the conclusions and recommendations.

CHAPTER TWO

LITERATURE REVIEW

2.1 Introduction

Different studies have been done to understand the behavior of stress sensitive formation. The effects of stress sensitivity were first shown by Dobrynin (1962). He investigated the effects of overburden pressure on some petrophysical properties of sandstone. He showed that pore compressibility is the main factor that contributes to the changes in permeability, porosity, resistivity and density. He used effective values that ranges from zero to 2500 psi for his experiments and found out that each of the petrophysical property measured can be characterized by maximum pore compressibility and effective stress. He also developed different equations that describe the physical behavior of each property.

Vairogs et al. (1971) showed that changes in formation characteristics due to stress in low permeability reservoirs could lead to a drop in its productivity. They carried out there study using a reservoir simulator. Vairogs and Rhoades (1973) showed that formation conductivity (kh) of gas well tests in stress-sensitive formations determined from conventional drawdown test analysis could be significantly in error when stress dependency of permeability is not taken into consideration.

Later studies were based on both pressure and rate transient analysis of stress sensitive formation. Samaniego & Cingo-Ley (1989) presented a practical procedure on for determining the stress dependent characteristics from transient pressure analysis using a conventional draw

down and build up analyses. The derived equations for both liquids and real gas flow by incorporating the pressure dependent variables as part of the characteristics into pseudopressure function.

Economides et al. (1974) a rate transient step pressure test to determine the permeability in stress sensitive reservoirs by measuring the flow rate changes with time at multiple constant bottomhole pressure.

Celis et al. (1994) developed type curves for analytical model for PTA in stress-sensitive naturally fractured reservoirs using the permeability modulus parameters as developed by Pedrosa (1986) for homogeneous (non- fractured) stress-sensitive porous media.

In other studies, it has been shown that clay plays an important part in permeability anisotropy. Neasham (1977) studied the effect of clay on permeability. He showed that the disperse clay morphology with the highest air permeability is predominantly the discrete particle. Dispersed clay morphology in the intermediate air permeability range is predominantly of a pore-lining variety. Hence, sands with pore-lining clays can have both significant amounts of clay and relatively good air permeability. The low permeability sandstones contain pore ridging clay morphology types. This bridging clay morphology forms partial to complete barriers to fluid flow and can seriously impair rock permeability, even for sand of relatively high porosity and low clay content.

More recently, Zahaf and Tiab (2002) investigated the effect of the presence of shale in sandstone formation on vertical and horizontal permeability anisotropy. They showed that permeability anisotropy is affected by both the volume fraction of shale and the shale type.

They also developed the following empirical equations that show the relationship between horizontal and vertical permeability. These equations are as follows:

1- Function of hydraulic mean radius:

$$k_v = A_1 \left(\sqrt{\frac{k_h}{\phi}} \right)^{B_1}$$

2- Function of clay content:

$$k_v = A_2 \left[(1-V_{sh}) \sqrt{\frac{k_h}{\phi}} \right]^{A_2}$$

3- Function of mean grain size:

$$k_v = A_3 \left(d_{gr} \sqrt{\frac{k_h}{\phi}} \right)^{B_3}$$

Where A_i and B_i are coefficients to be determined for a specific field case.

2.2 Effect of Stress on Permeability

The effect of overburden stress on petrophysical properties of rock such as permeability, porosity, resistivity and density, was extensively investigated by Dobrynin. He concluded that the main factor that contributes to the change in these petrophysical properties is due to the pore compressibility, which, in the range of 0 to 20,000 psi, can be characterized by the maximum pore compressibility and effective stress (i.e. $\sigma_{eff} = \sigma_{ob} - aP_p$ where a is called

effective stress coefficient). He also developed several general equations that describe the behavior of the physical properties of sandstone under pressure.

The stress in the formation can cause the strain of the porous medium, which will affect the porosity and the permeability. The state of stress in a porous medium has been treated by Lubinski and more recently by Deily and Owens (Vairog, 1971). Strains in a porous medium subjected to formation stresses and pore pressure are as follows:

$$\varepsilon_r = \frac{1}{E}[\sigma_r - \nu(\sigma_\theta + \sigma_z)] + \frac{1-2\nu}{E}(1 - \delta - \phi)P_p \quad \text{..... (2.1)}$$

$$\varepsilon_\theta = \frac{1}{E}[\sigma_\theta - \nu(\sigma_r + \sigma_z)] + \frac{1-2\nu}{E}(1 - \delta - \phi)P_p \quad \text{..... (2.2)}$$

$$\varepsilon_z = \frac{1}{E}[\sigma_z - \nu(\sigma_r + \sigma_\theta)] + \frac{1-2\nu}{E}(1 - \delta - \phi)P_p \quad \text{..... (2.3)}$$

Where,

$$\delta = \frac{(1-2\nu_m)/E_m}{(1-2\nu)/E}$$

Palmer and Mansoori (1998) derived an equation that relates porosity, strain, moduli and pressure. This relationship is shown in Equation 2.4 as follows.

$$\frac{\phi}{\phi_0} = 1 + \frac{C_m}{\phi_0}(p - p_0) + \frac{\varepsilon_l}{\phi_0}\left(\frac{K}{M} - 1\right) \times \left(\frac{\beta p}{1+\beta p} - \frac{\beta p_0}{1+\beta p_0}\right) \quad \text{..... (2.4)}$$

Where,

$p - p_0$ = Pressure drawdown and ε_l, β = parameters of Langmuir curve match to volumetric strain change because of matrix shrinkage (ε_l, dimensionless and β is psi^{-1})

The moduli, M and K are independent of pressure, as can be seen from the laboratory results of Zheng *et al.* (1991), and the relationship of c_m is as follows:

$$c_m = \frac{1}{M} - \left[\frac{K}{M} + f - 1\right]\gamma \qquad \text{..... (2.5)}$$

Based on the above functions, the changes in porosity can be calculated as functions of elastic moduli, initial porosity, sorption isotherm parameters, and pressure drawdown.

According to Dobrynin, between a certain minimum net overburden pressure P_m and a certain maximum net overburden pressure P_M the relation between pore compressibility and the logarithm of pore pressure can be approximated by a straight line, which can be expressed mathematically as follows:

$$c_p = \frac{c_{pMax}}{\log(p_M/p_m)}\log(P_M/P) \qquad \text{..... (2.6)}$$

Where C_{pMax} = maximum pore compressibility

The change in permeability is mainly due to the contraction of the pore channels. The permeability of the formation decreases with the increasing values of stress. Dybrynin derived the following semi-empirical equation:

$$\frac{\Delta k}{k} = 2\left(1 + f_{ps}\right)C_{pMax}f(P) \qquad \text{..... (2.7)}$$

Where $f(P) = P_m + \frac{P}{log\frac{P_M}{P_m}}\left[log\frac{P_M}{P} + 0.434 - \frac{P_m}{P}\left(log\frac{P_M}{P_m} + 0.434\right)\right]$ and f_{ps} is the pore shape factor. The permeability decrease rapidly at low stress and stabilizes with increasing confining or overburden stress as shown in the figure 2.1.

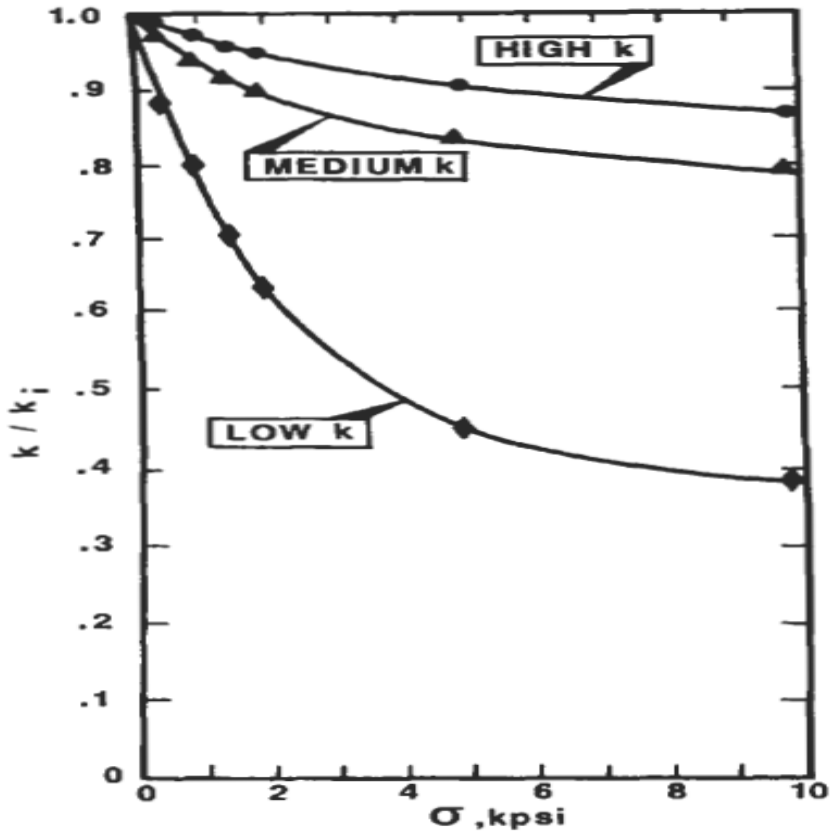

Figure 2.1 - Variation of permeability with stress (Tiab 2004).

CHAPTER THREE

UNDERLYING THEORY OF PERMEABILITY RELATIONSHIPS

3.1 Introduction

It is well-documented in literatures that permeability of a formation depends on its grain size, grain distribution and shape; pore throat size, distribution and shape; and clay content, clay type and clay distribution.

Permeability-porosity relationship was first developed by Kozeny (1927) and then modified by Carman (1939). The modified Kozeny-Carman equation is

$$k = \frac{{\phi_e}^3}{(1-\phi_e)^2}\left[\frac{1}{F_{ps}*\tau^2*{S_{gv}}^2}\right] \quad \text{..... (3.1)}$$

Where k = permeability

ϕ_e = effective porosity

F_{ps} = 3-D pore shape factor

τ = tortuosity

S_{gv} = specific surface area per unit volume

Dividing the equation above and taking square root of both sides results in

$$\sqrt{\frac{k}{\phi_e}} = \frac{\phi_e}{1-\phi_e} * \left[\frac{1}{F_{ps}*\tau*S_{gv}}\right] \quad \text{..... (3.2)}$$

$\sqrt{\frac{k}{\phi_e}}$ is called the mean hydraulic radius

It was shown that the mean hydraulic radius can be correlated to various petrophysical parameter (Amaefule et al.). This led to the concept of hydraulic flow unit and rock typing. Taking k in equation 3.2 to be horizontal permeability and correlating the horizontal mean hydraulic radius with vertical permeability yields the following relationship:

$$k_v = A_1 * \left(\sqrt{\frac{k_h}{\phi_e}}\right)^{B_1} \quad \text{..... (3.3)}$$

Where A_1 and B_1 are constants.

3.2 A New Permeability Relationship for Shaly Formation

For shaly formations, the clay content, clay type and clay distribution affect both the value of horizontal and vertical permeability by reducing the pore volume and thereby reducing the effective porosity. Removing the effect of shale volume from the effective porosity gives the effective porosity with respect to the sum of pore and matrix volume i.e.

$$\phi_e{}' = \frac{\phi_e}{1 - V_{sh}}$$

Substituting into equation 3 gives:

$$k_v = A_2 * \left(\sqrt{\frac{k_h(1-V_{sh})}{\phi_e}}\right)^{B_2} \quad \text{..... (3.4)}$$

The effect of the clay type and distribution would affect the value of the two constants, hence, A_1 and B_1 becomes A_2 and B_2 constants.

Also, by multiplying both sides of equation 3.1 with ϕ_e and taking square root of both sides results in:

$$\sqrt{k\phi_e} = \phi_e * \sqrt{\frac{k}{\phi_e}} = \frac{{\phi_e}^2}{1-\phi_e} * \left[\frac{1}{F_{ps}*\tau*S_{gv}}\right] \quad \text{..... (3.5)}$$

Taking k in equation 3.5 to be horizontal permeability and correlating vertical permeability with the product of effective porosity and horizontal mean hydraulic radius yields the following relationship

$$k_v = A_3 \left(\phi_e * \sqrt{\frac{k_h}{\phi_e}}\right)^{B_3} \quad \text{..... (3.6)}$$

$$k_v = A_3 \left(\sqrt{k_h \phi_e}\right)^{B_3} \quad \text{..... (3.7)}$$

$$k_v = A_3 (k_h \phi_e)^{\frac{B_3}{2}} \quad \text{..... (3.8)}$$

Equation 3.6, 3.7 and 3.8 are the same but are arranged differently

For shaly formation, applying the same concept applied in the derivation of equation 3.4 to equations 3.6, 3.7 and 3.8 results in

$$k_v = A_4 \left(\frac{\phi_e}{1-V_{sh}} * \sqrt{\frac{k_h(1-V_{sh})}{\phi_e}}\right)^{B_4} \quad \text{..... (3.9)}$$

$$k_v = A_4 \left(\sqrt{\frac{k_h \phi_e}{1 - V_{sh}}} \right)^{B_4} \quad \text{..... (3.10)}$$

$$k_v = A_4 \left(\frac{k_h \phi_e}{1 - V_{sh}} \right)^{\frac{B_4}{2}} \quad \text{..... (3.11)}$$

In addition, equation 3.9, 3.10 and 3.11 are the same but are arranged in different forms.

CHAPTER FOUR

SAMPLE FIELD DATA CASES

4.1 Introduction

Different field cases were analyzed to derive the best relationship between vertical and horizontal permeability for each field scenario. Three field cases were analyzed. A Nigerian field, an Iranian field and a Saudi Arabian field were used for this study. The Nigerian reservoir represents a sandstone case while the other two represents both limestone and dolostone cases of carbonate systems.

4.2 Sandstone Field Case

Sandstone reservoirs are not as stress sensitive as carbonate reservoirs. There petrophysical properties are mostly controlled by depositional processes. They are mostly not as heterogeneous as their carbonate counterparts are. They are relatively easier to characterize, as they are mostly not affected by post depositional attributes. Different relationships between vertical permeability and other petrophysical parameters exist for sandstone formation. This study compares some of this correlations with that of a carbonate formation to investigate and establish the best correlation for each case.

4.2.1 Field Description of a Nigerian Sandstone Case

The field was formed during the tertiary period and is made up of seven different reservoir facies with shale intercalations. The facies were described from the core taken from the

reservoir. The facies that where identified include the transgressive sands, tidal channels, tidal flats, point bars, upper and lower shore faces. The reservoir is layered with vertical heterogeneity. The log data and drilling operation confirmed the presence of gas in the reservoir. The porosity was calculated from the well log and calibrated with the lab measured core porosity. Permeability was measured in the lab.

4.3 Carbonate Field Cases

Most carbonate reservoirs are naturally fractured. They contain fractures that can range from isolated microscopic fissures to kilometer-long structures called fracture swarms or corridors. The fractures create complex paths for hydrocarbons and other fluids, which affect reservoir characterization, production performance, and ultimate recovery. In addition, because of the presence of the fractures, the carbonate formations are very sensitive to the changing of stress because of the elasticity of rock and large pressure changes can cause significant changes in fracture apertures.

Unlike sandstones, with their well-characterized correlations of porosity, permeability, and other reservoir properties, the heterogeneous pore and fracture systems of carbonate rocks most times defy routine petrophysical analysis. Moreover, in the naturally fractured carbonate formations, permeability changes spatially and temporally due to production and injection processes (Lorenz 1999). Therefore, it is relatively complicated to investigate the correlations in the carbonate formations. However, after analysis of the data, some comparatively simple relationships that might have existed between depositional attributes, porosity, and permeability are obscured by these multiple physical, biological, and chemical influences,

operating at different scales, during and continuing after deposition. This study recognizes a general relationship between horizontal and vertical permeability in this field. The relationship was obtained by reviewing wells in which both horizontal and vertical permeability was available from core analysis.

4.3.1 Field Description of an Iranian Carbonate Case

The field has an estimated area of 1200 square kilometers. The field is predominantly a gas field and the average thickness of the gas column in the reservoir analyzed is approximately 300m. Estimated initial gas in place was 25TCF. The reservoir consists mainly of limestone and dolomite layer with minor anhydrite. The first well drilled in the reservoir started in October 1997 and reached a total vertical depth of 3345m. The gas reservoir produces 17 STB of condensate for every million SCF of gas produced. The porosity and the permeability measurement were taken from available routine core data from wells in the reservoir.

4.3.2 Field Description of a Saudi Arabian Carbonate Case

A stress-sensitive naturally fractured carbonate formation of an oil field in Saudi Arabia was also chosen for investigating the vertical - horizontal permeability relationship as well as other relationships. The reservoir layers range from 3000 to 3260 ft. Rock strength data from cores and logs of one well from this field were analyzed. The depositional environment of this carbonate reservoir contains numerous facies changes, as well as reservoir extension. The reservoir facies vary in quality because of their diagenetic history. They are usually multi-layered producing zones. The carbonate formation can be divided into 5 different layers with

respect to their lithology. The limestone units are approximately from 3055 to 3080 ft. and 3220 to 3260 ft., the total thickness is around 70 ft. Some parts of the carbonate reservoir facies have been dolomitized and later leached which resulted in good reservoir development. In addition, the dolomite units are from 3000 ft. to 3050 ft. and 3085 to 3165 ft., the total thickness is above 130 ft. Other layers are shaly or shale layers.

This formation is a prolific producer of oil and gas but its porosity and permeability distribution are complex and primarily controlled by the depositional facies distribution and its fractures are produced by mechanical stresses during the later diagenesis or fracturing process. The porosity varies from about 30% to less than 5%, while the permeability ranges from 400 mD to less than 10 mD.

CHAPTER FIVE

RESULT AND DISCUSSION

5.1 Introduction

Most of the reservoir engineering concepts are based on homogenous reservoirs despite the fact that the homogenous reservoirs are the exceptions. This is especially true for most of the carbonate reservoirs. The reservoir sections studied in this work were considered heterogeneous. The pattern of variation of permeability with depth for the wells shows that the reservoirs are heterogeneous.

In the wireline logs used in this study, the gamma ray log coupled with the density log and neutron log were used to identify the shale fractions. The lowest point on the gamma ray log is considered the clean formation point. A higher gamma ray value signifies higher clay content since the clay particles emit radiation as a function of clay volume. Sections of uniform grain density and low gamma ray readings were chosen as layers to be analyzed.

Using the values from the gamma ray log, the shale volume can be estimated. A correlation for tertiary rocks less than 4,000 ft. in depth is given by:

$$V_{sh} = 0.083(2^{3.7I_{sh}} - 1) \quad \text{..... (5.1)}$$

The gamma ray index, I_{sh}, is defined as:

$$I_{sh} = \frac{GR - GR_{CS}}{GR_{sh} - GR_{CS}} \quad \text{..... (5.2)}$$

Where GR is the value of the gamma ray log at the area being analyzed, GR_{CS} is the gamma ray value for clean sand (this is generally taken as the lowest value on the gamma ray curve); GR_{sh} is the gamma ray value from a shale zone.

For older rocks (4,000 to 8,000 ft. deep):

$$V_{sh} = 0.33(2^{2I_{sh}} - 1) \quad \text{..... (5.3)}$$

For very hard compacted formation (at a depth of 8,000 ft. or more), $V_{sh} = I_{sh}$

5.2 Data Analysis

5.2.1 Niger-Delta Sandstone Case

This zone was easily identified and characterized from wireline log and core data. The depth of the zone ranges from 11850 ft. to 12150 ft. and is made up of at least seven different discrete rock types. The average grain density of the layers is 2.66g/cm^3. The variation of vertical and horizontal permeability with depth and effective porosity are shown in figures 5.1, 5.2, 5.3 and 5.4 respectively. It could be seen from figures 5.1 and 5.2 that both horizontal and vertical permeability generally decreases with increase in depth. Also figures 5.3 and 5.4 shows a semi log relationship between effective porosity and permeability in both horizontal and vertical directions. Combining both relationships in figure 5.3 and 5.4 yields a relationship between vertical and horizontal permeability.

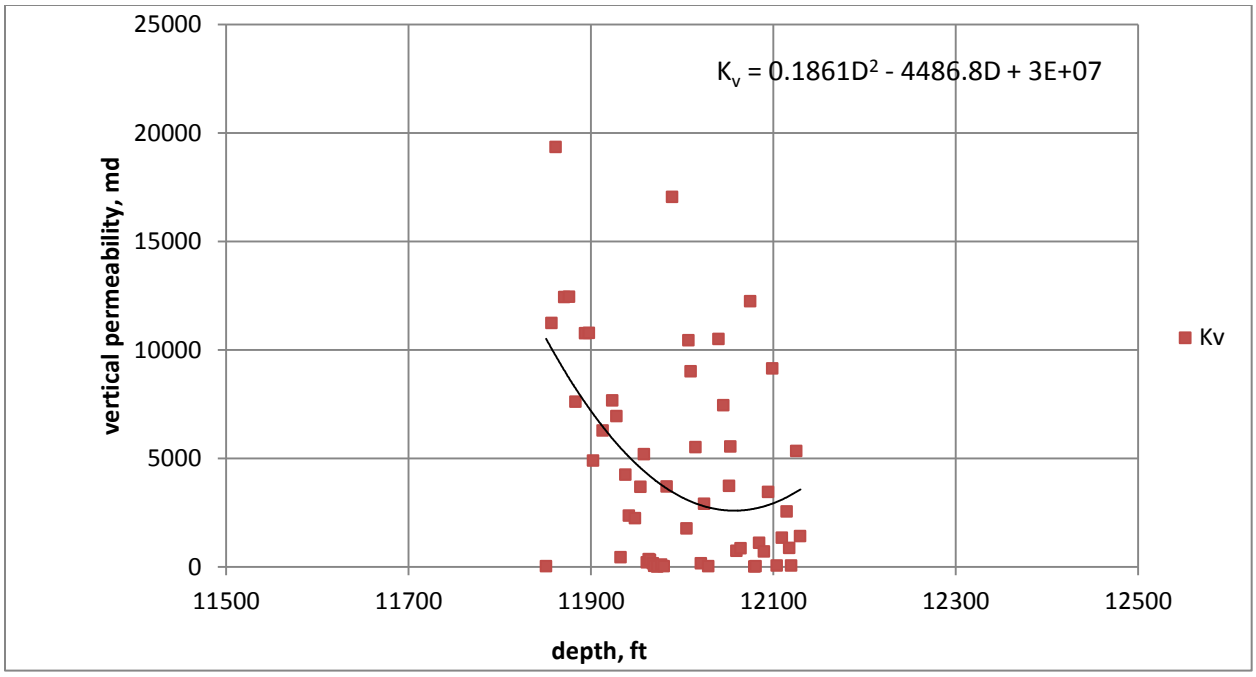

Figure 5.1- Variation of vertical permeability with depth for Niger-Delta sandstone case.

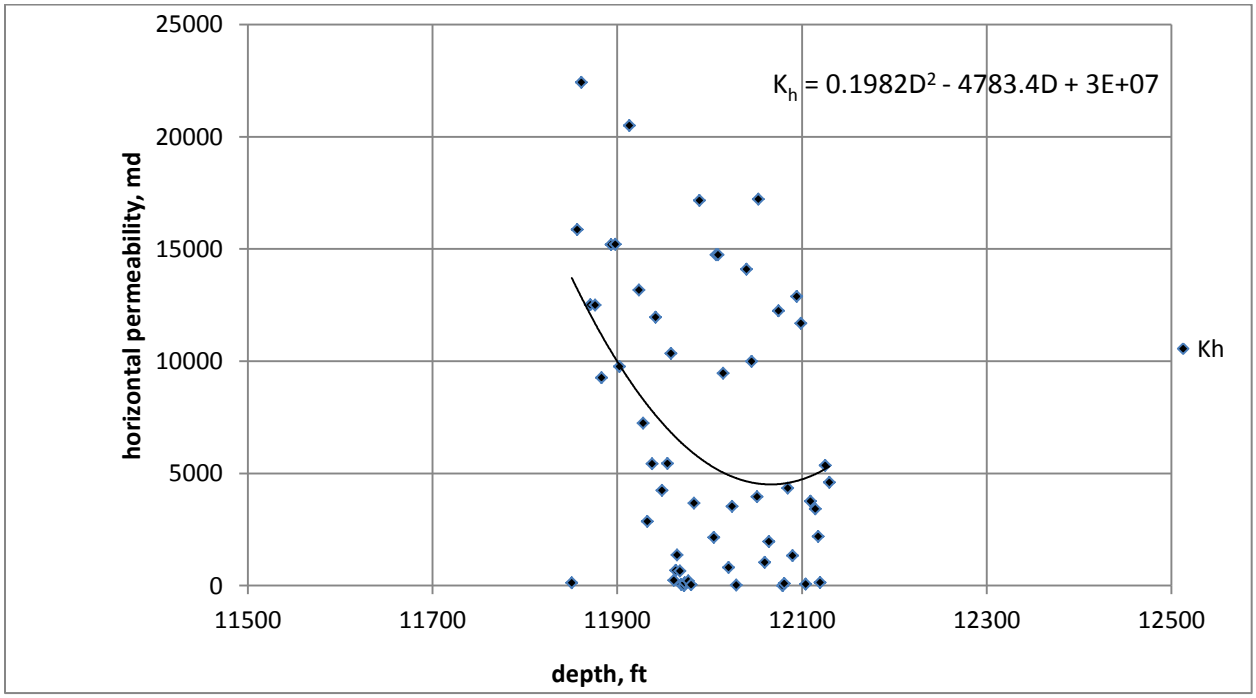

Figure 5.2- Variation of horizontal permeability with depth for Niger-Delta sandstone case.

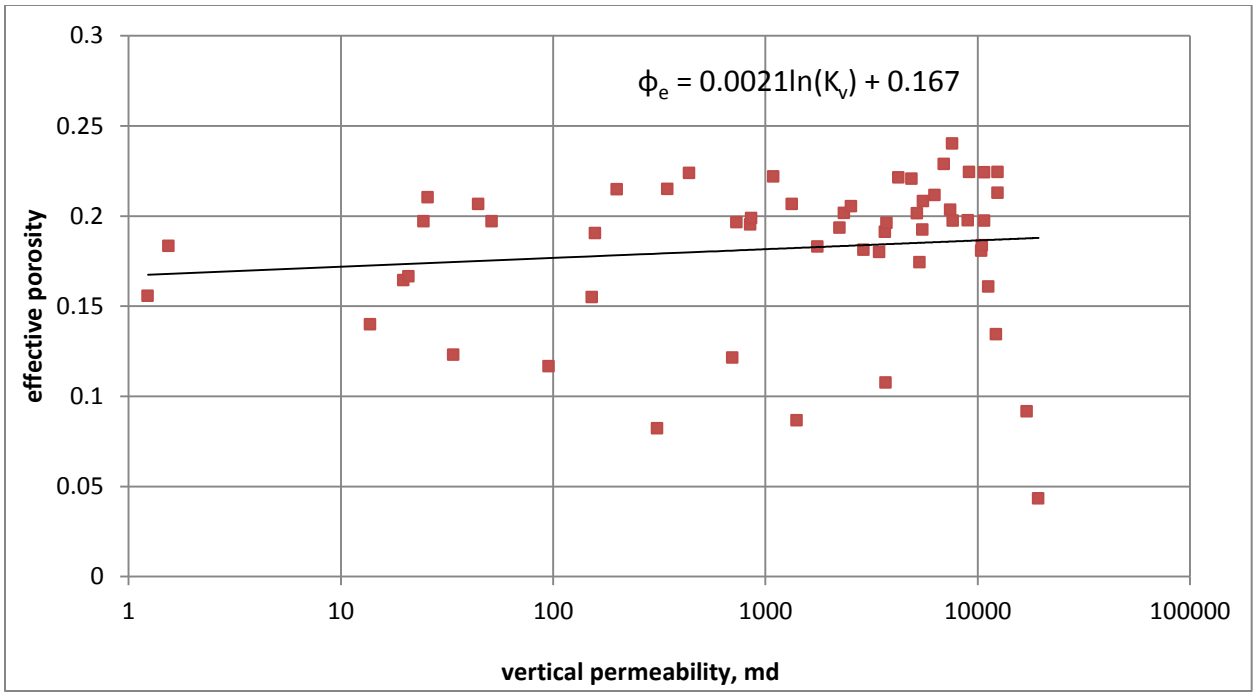

Figure 5.3- Variation of vertical permeability with effective porosity for Niger-Delta sandstone case.

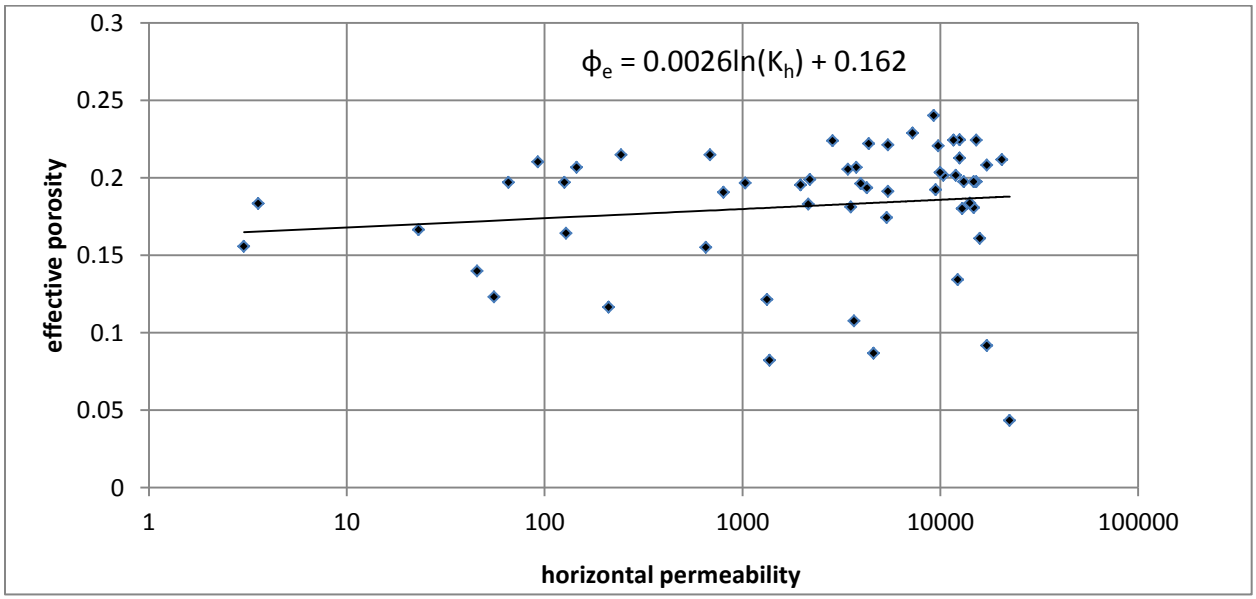

Figure 5.4- Variation of horizontal permeability with effective porosity for Niger-Delta sandstone case.

By plotting the vertical permeability and horizontal permeability on a log-log graph, we get the following correlation with a correlation coefficient of 0.9543 (see figure 5.5):

$$k_v = 0.2997 k_h^{1.0707} \quad \text{..... (5.4)}$$

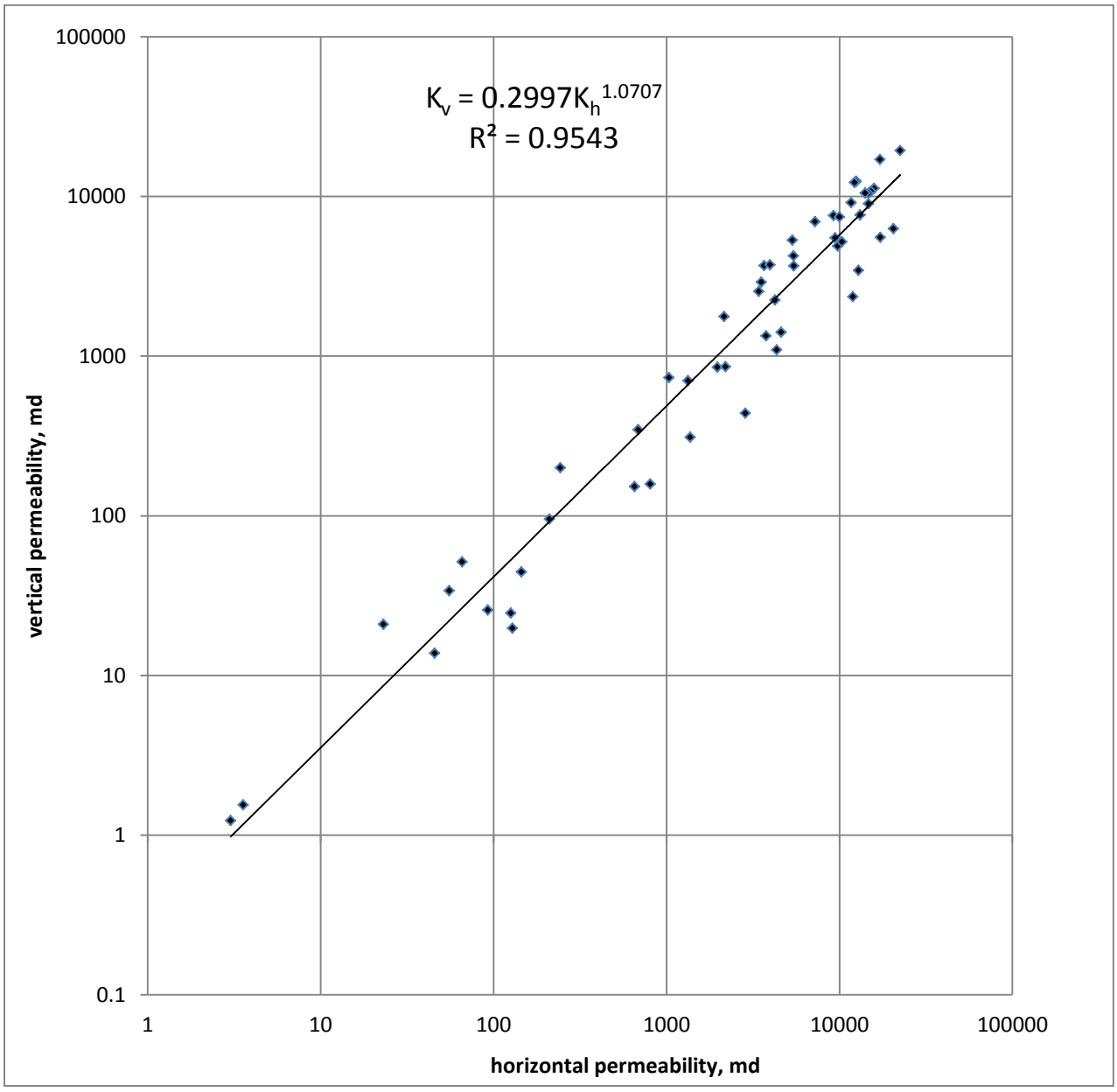

Figure 5.5- Variation of vertical permeability with horizontal permeability for Niger-Delta sandstone case.

The range of the permeability anisotropic ratio, i.e. k_v/k_h, is from 0.15 to 1.0 and is shown in the Figure 5.6. The variation of effective porosity with the anisotropy permeability ratio is shown in Figure 5.7.

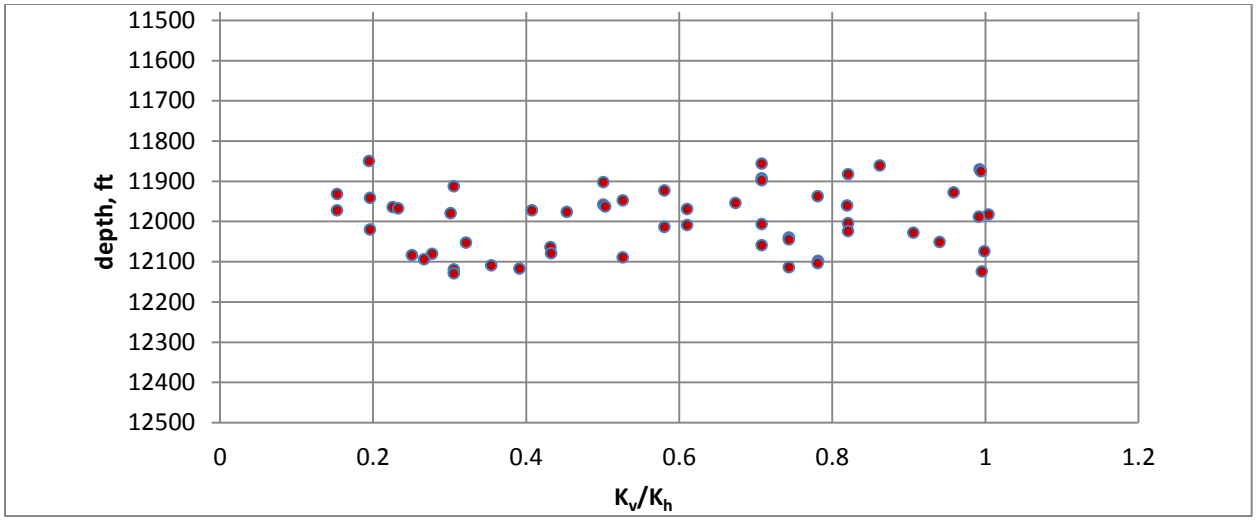

Figure 5.6- Variation of anisotropic permeability ratio with depth for the Niger-Delta sandstone case.

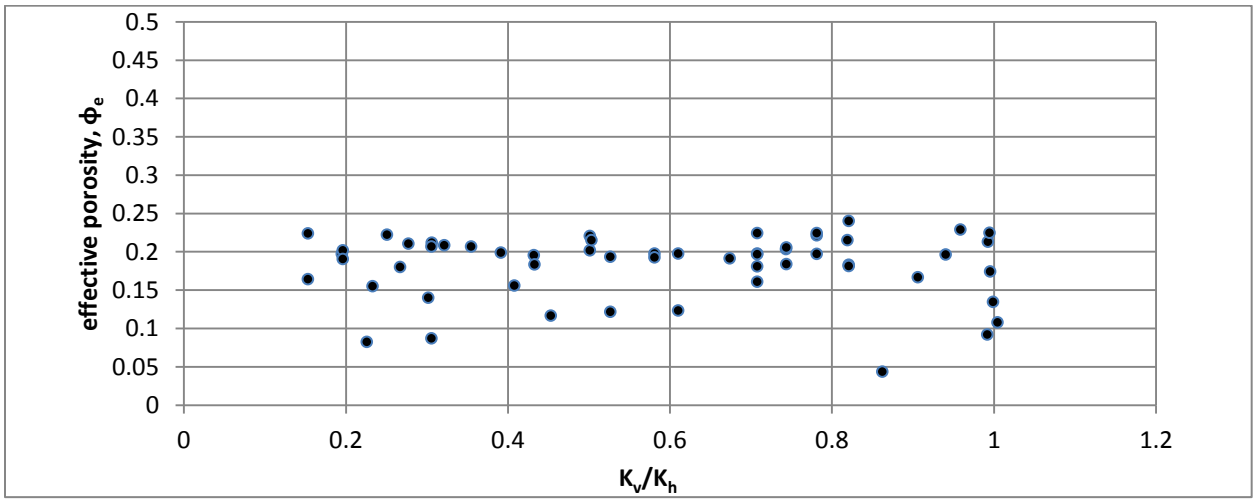

Figure 5.7- Variation of anisotropic permeability ratio with effective porosity for the Niger-Delta sandstone case.

The variations of vertical permeability with other parameters are shown in Figure 5.8 through 5.13.

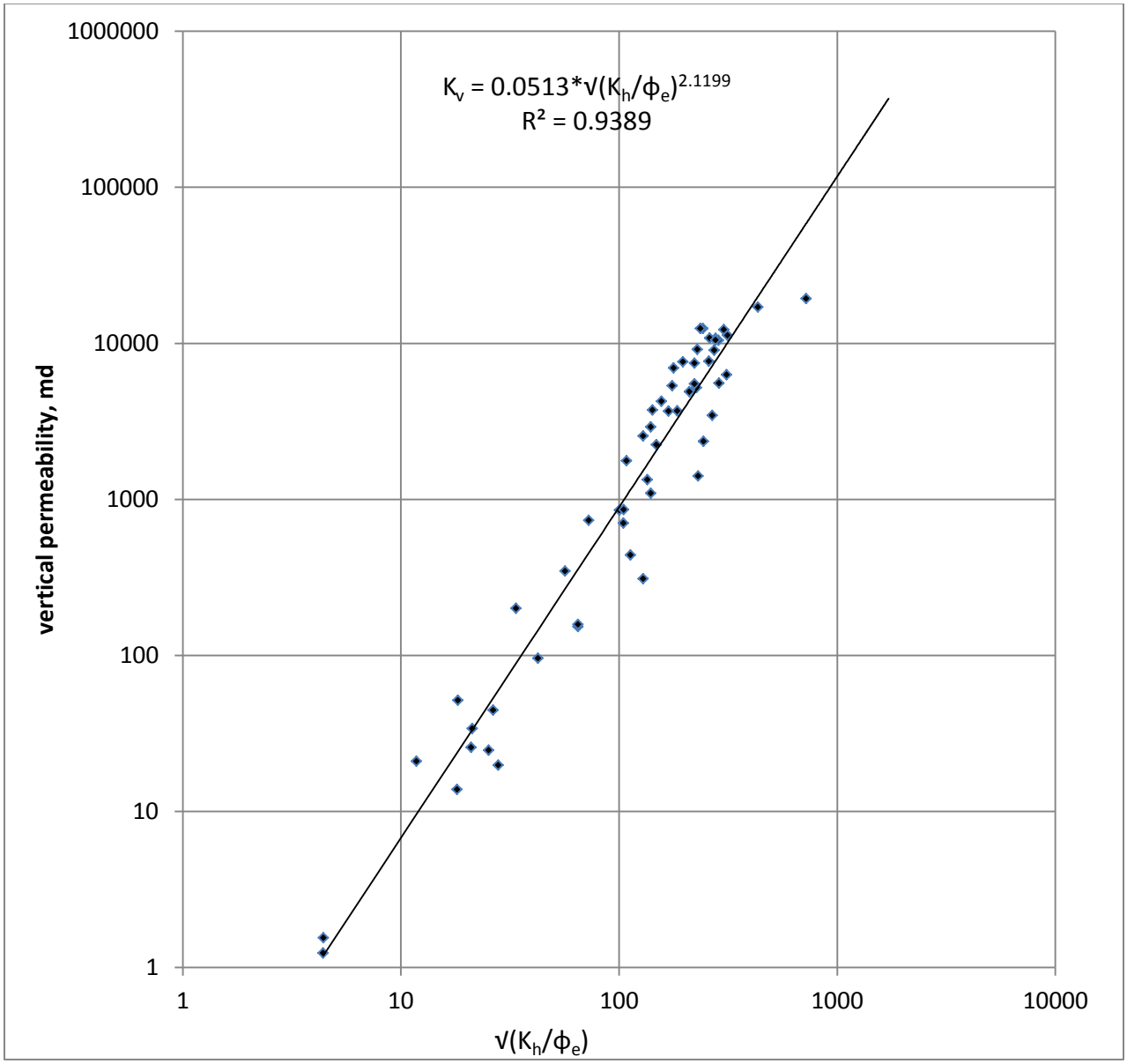

Figure 5.8- Variation of vertical permeability with mean hydraulic radius for the Niger-Delta sandstone case.

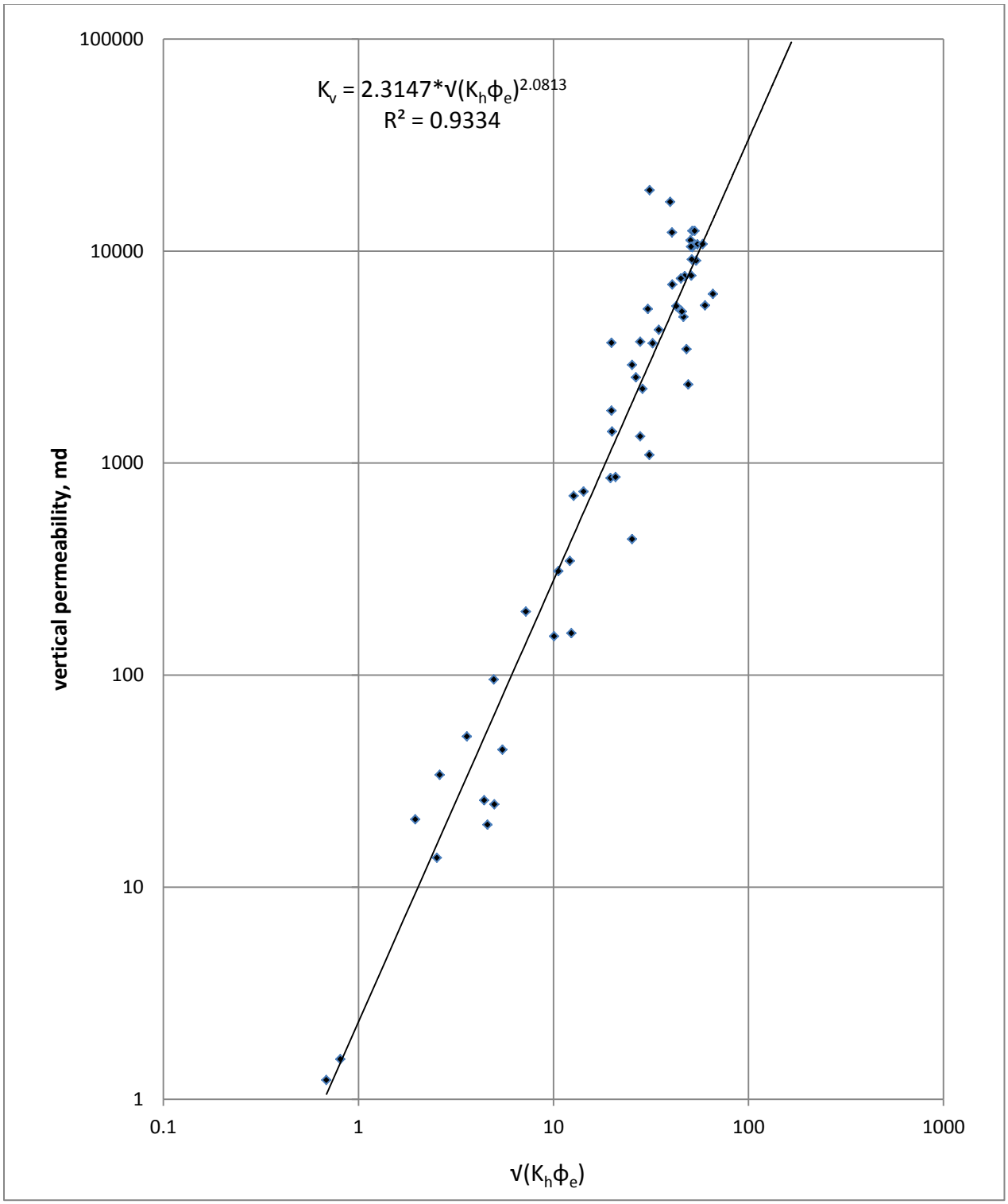

Figure 5.9- Variation of vertical permeability with $\sqrt{K_h\phi_e}$ for the Niger-Delta sandstone case.

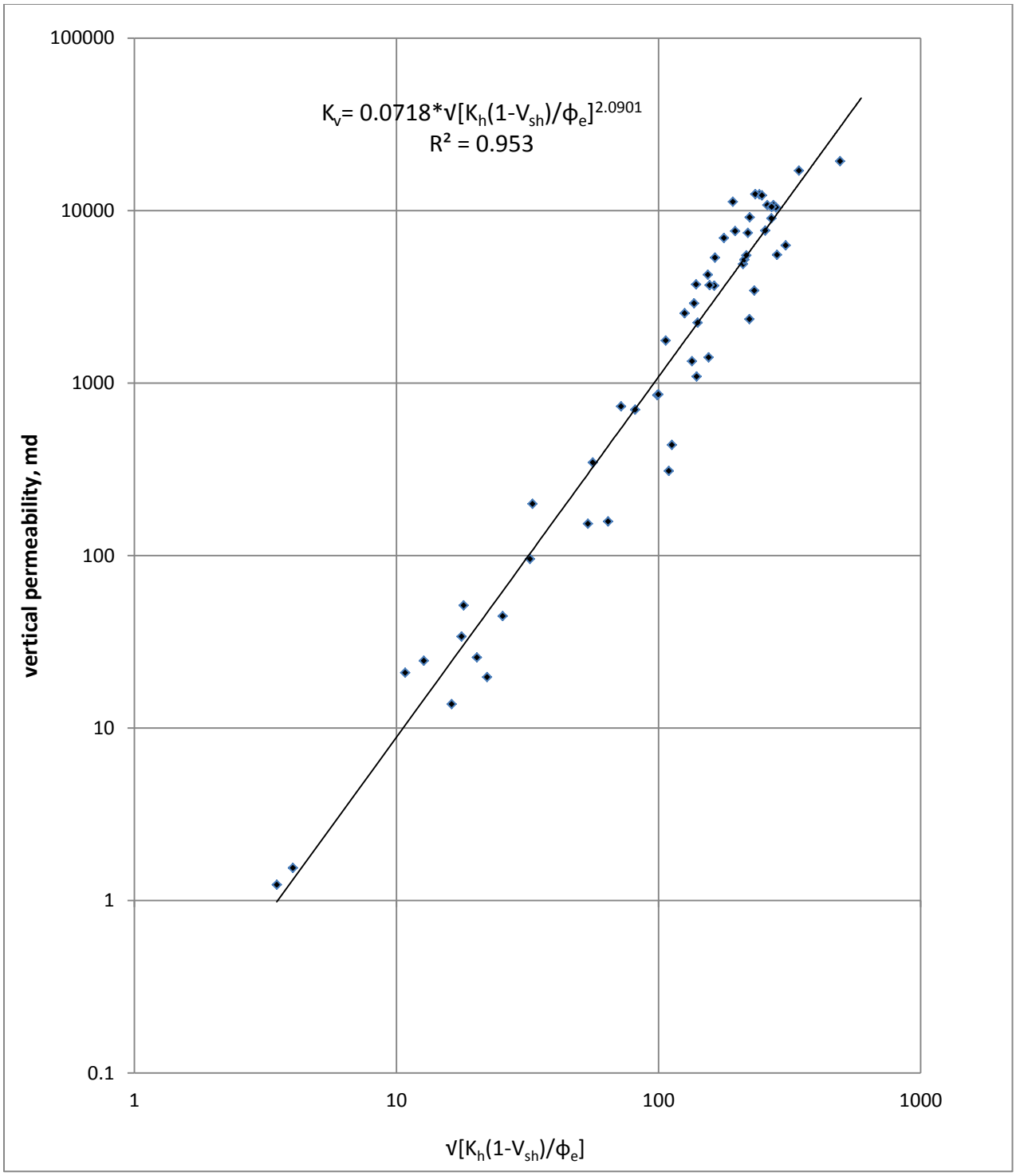

Figure 5.10- Variation of vertical permeability with $\sqrt{K_h(1-V_{sh})/\phi_e}$ for the Niger-Delta sandstone case.

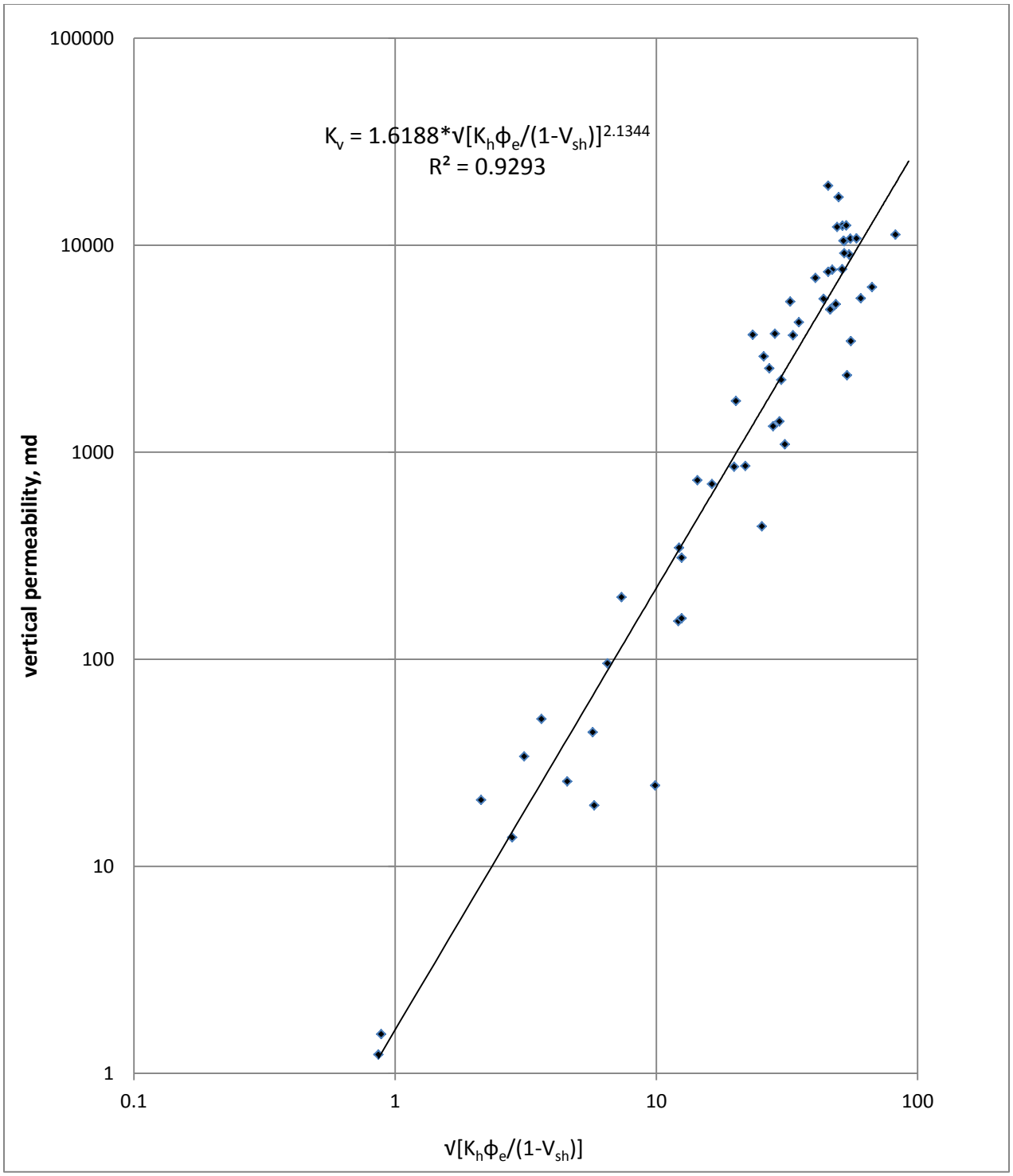

Figure 5.11- Variation of vertical permeability with $\sqrt{K_h\phi_e/(1-V_{sh})}$ for the Niger-Delta sandstone case.

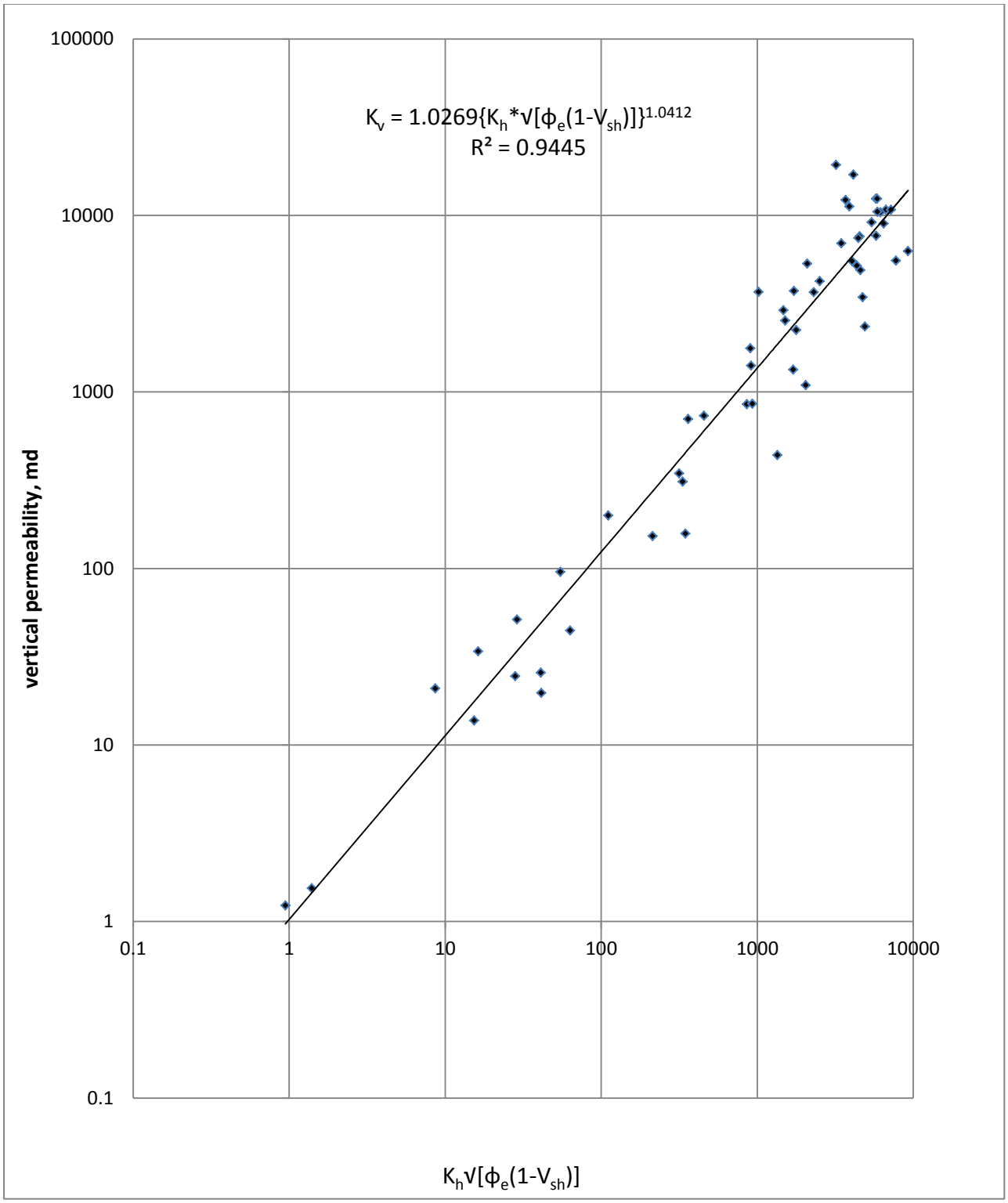

Figure 5.12- Variation of vertical permeability with $K_h * \sqrt{\phi_e(1 - V_{sh})}$ for the Niger-Delta sandstone case.

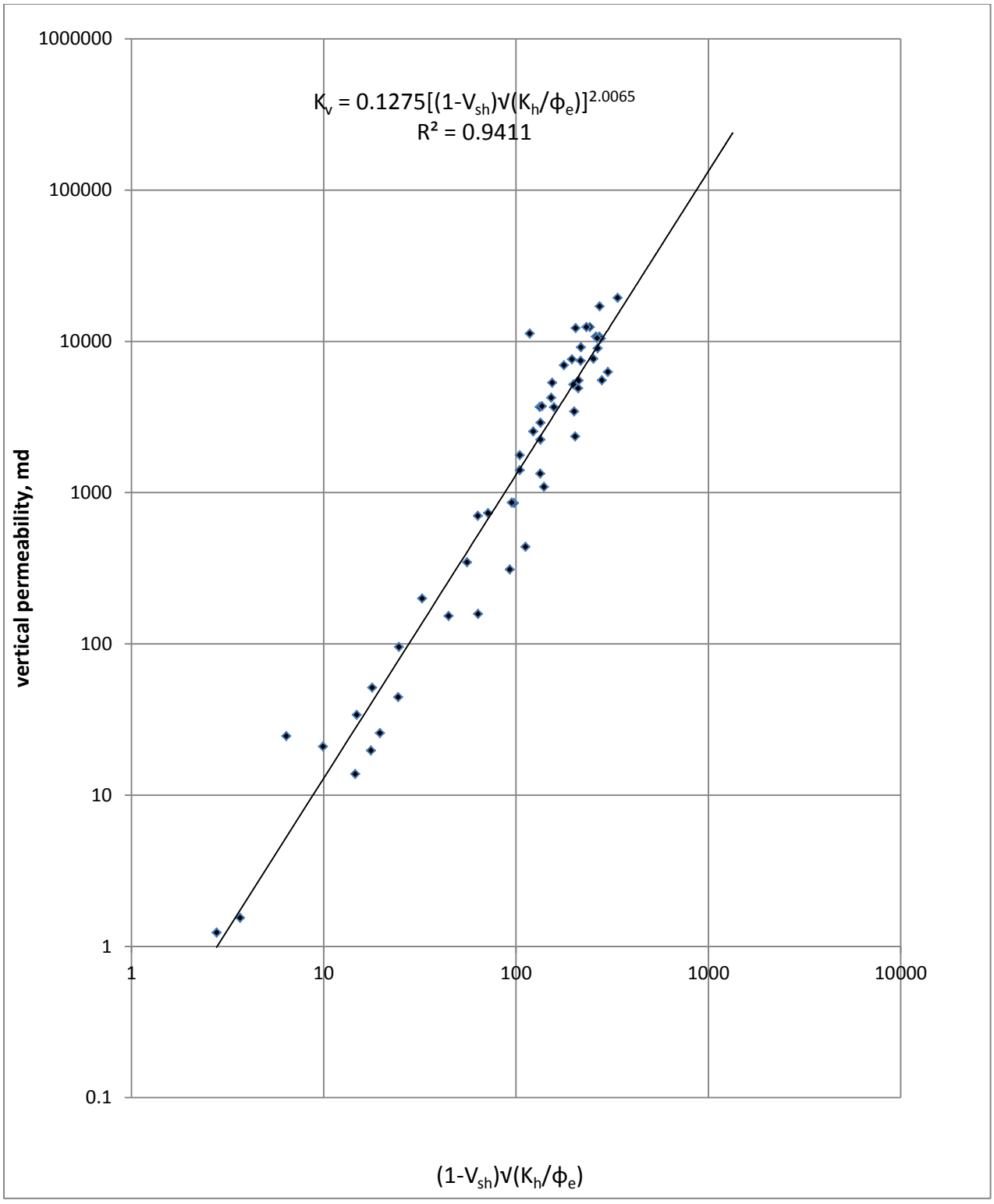

Figure 5.13- Variation of vertical permeability with $(1 - V_{sh})\sqrt{k_h/\phi_e}$ for the Niger-Delta sandstone case.

From figure 5.8 through 5.13, the following correlations are obtained:

$$k_v = 0.0513\left(\sqrt{\frac{k_h}{\phi_e}}\right)^{2.1199} \quad (R^2 = 0.9389) \quad \text{..... (5.5)}$$

$$k_v = 2.3147\left(\sqrt{K_h\phi_e}\right)^{2.0813} \quad (R^2 = 0.9334) \quad \text{..... (5.6)}$$

$$k_v = 0.0718\left[\sqrt{K_h(1-V_{sh})/\phi_e}\right]^{2.0901} \quad (R^2 = 0.953) \quad \text{..... (5.7)}$$

$$k_v = 1.6188\left[\sqrt{\frac{k_h\phi_e}{(1-V_{sh})}}\right]^{2.1344} \quad (R^2 = 0.9293) \quad \text{..... (5.8)}$$

$$k_v = 1.0269\left[k_h * \sqrt{(1-V_{sh})\phi_e}\right]^{1.0412} \quad (R^2 = 0.9445) \quad \text{..... (5.9)}$$

$$k_v = 0.1275\left[(1-V_{sh})\sqrt{\frac{k_h}{\phi_e}}\right]^{2.0065} \quad (R^2 = 0.9411) \quad \text{..... (5.10)}$$

The conventional vertical-horizontal permeability plot as shown in figure 5.5 may not always yield meaningful relationship, but equations 5.5 through 5.10 provide an excellent method of analysis i.e. relating k_v to k_h by combining porosity and shaliness of the formation.

The effective stress is found out from the following equation:

$$\sigma_e = 0.572D \quad \text{..... (5.11)}$$

The value of pore compressibility c_p is calculated using the following formula

$$\bar{c}_p = \frac{c_o}{\alpha\Delta\sigma}(1 - e^{-\alpha\Delta\sigma}) \quad \text{..... (5.12)}$$

Matrix compressibility is found out from the following relationship

$$c_r = \phi c_P \quad \text{..... (5.13)}$$

The bulk modulus is the reciprocal of the matrix compressibility, i.e.

$$K = \frac{1}{c_r} \quad \text{..... (5.14)}$$

Since Poisson's ratio of 0.25 holds good for most of the formation, this value is used to find out the Young's Modulus from the following equation.

$$K = \frac{E}{3(1-2\nu)} \quad \text{..... (5.15)}$$

5.2.1 Iranian Carbonate Case

This zone was identified and characterized from well logging and core data. The depth of this zone ranges from 10550 ft. to 10975 ft. The average grain density for the layer analysed is 2.71g/cm^3. This layer contains little or no shale therefore the shale fraction was taken to be zero. The reservoir was characterized using the hydraulic flow unit concept. The flow units were then divided into discrete rock types (DRT). The vertical permeability correlations that were

developed for this reservoir were for a single DRT. Other DRTs for this reservoir shows similar vertical permeability correlations. The variation of vertical and horizontal permeability with effective porosity is shown in Figures 5.14 and 5.15 respectively.

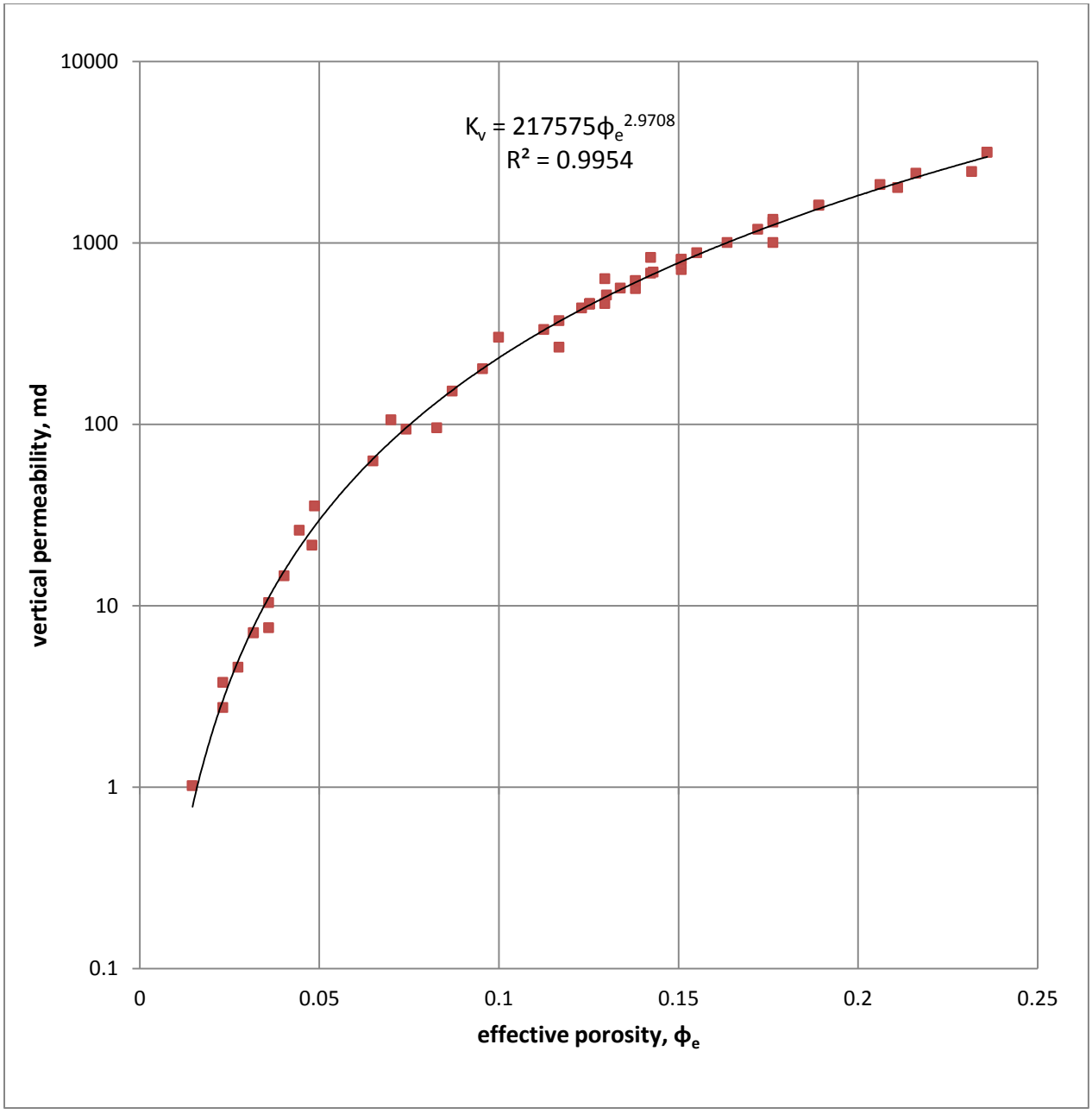

Figure 5.14- Variation of vertical permeability with effective porosity for the DRT of the Iranian carbonate case.

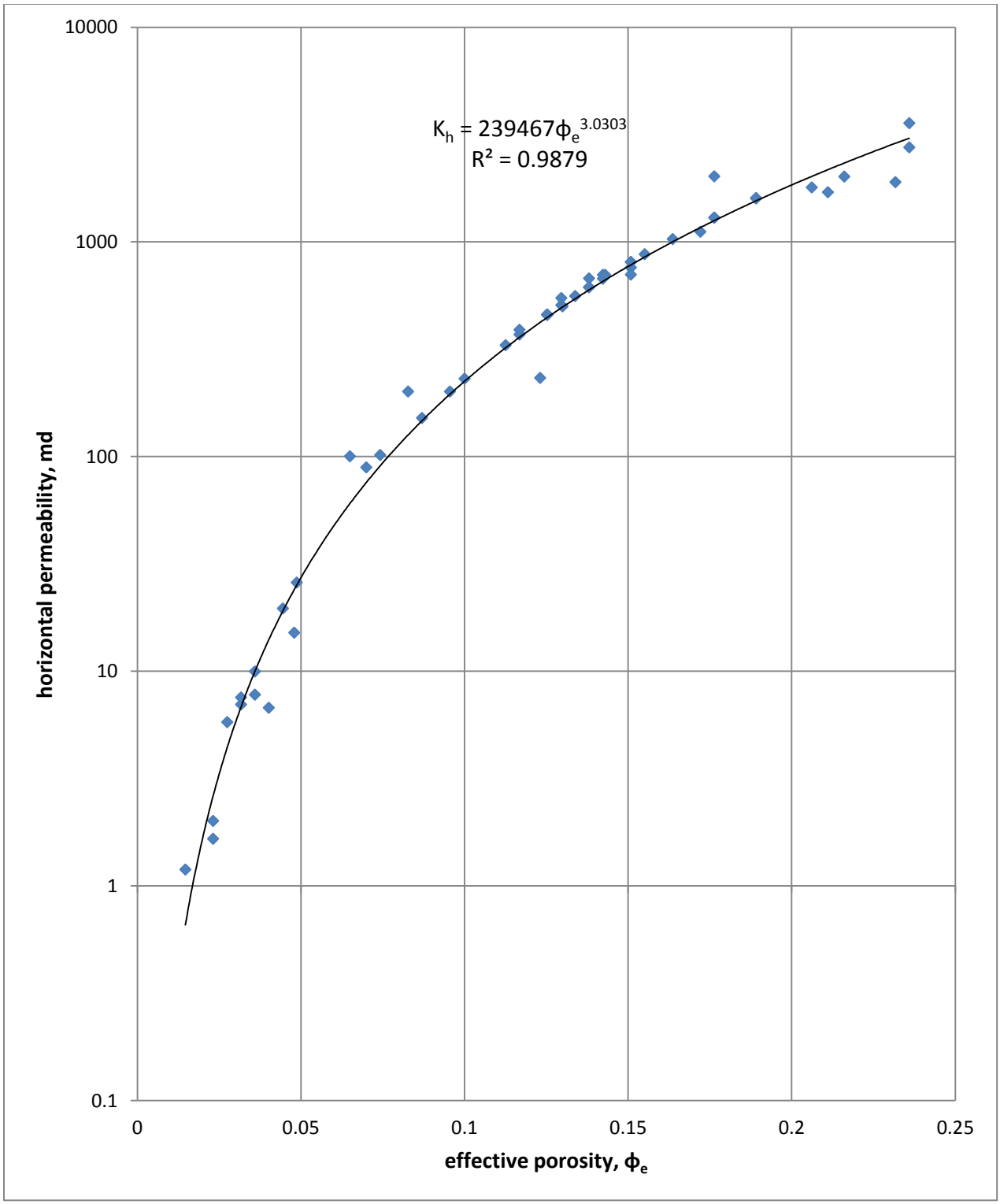

Figure 5.15- Variation of horizontal permeability with effective porosity for the DRT of the Iranian carbonate case.

By plotting the vertical permeability and horizontal permeability on a log-log graph, we get the following correlation with a correlation coefficient of 0.9853 (see figure 5.16):

$$k_v = 1.226k_h^{0..9701} \quad \text{..... (5.16)}$$

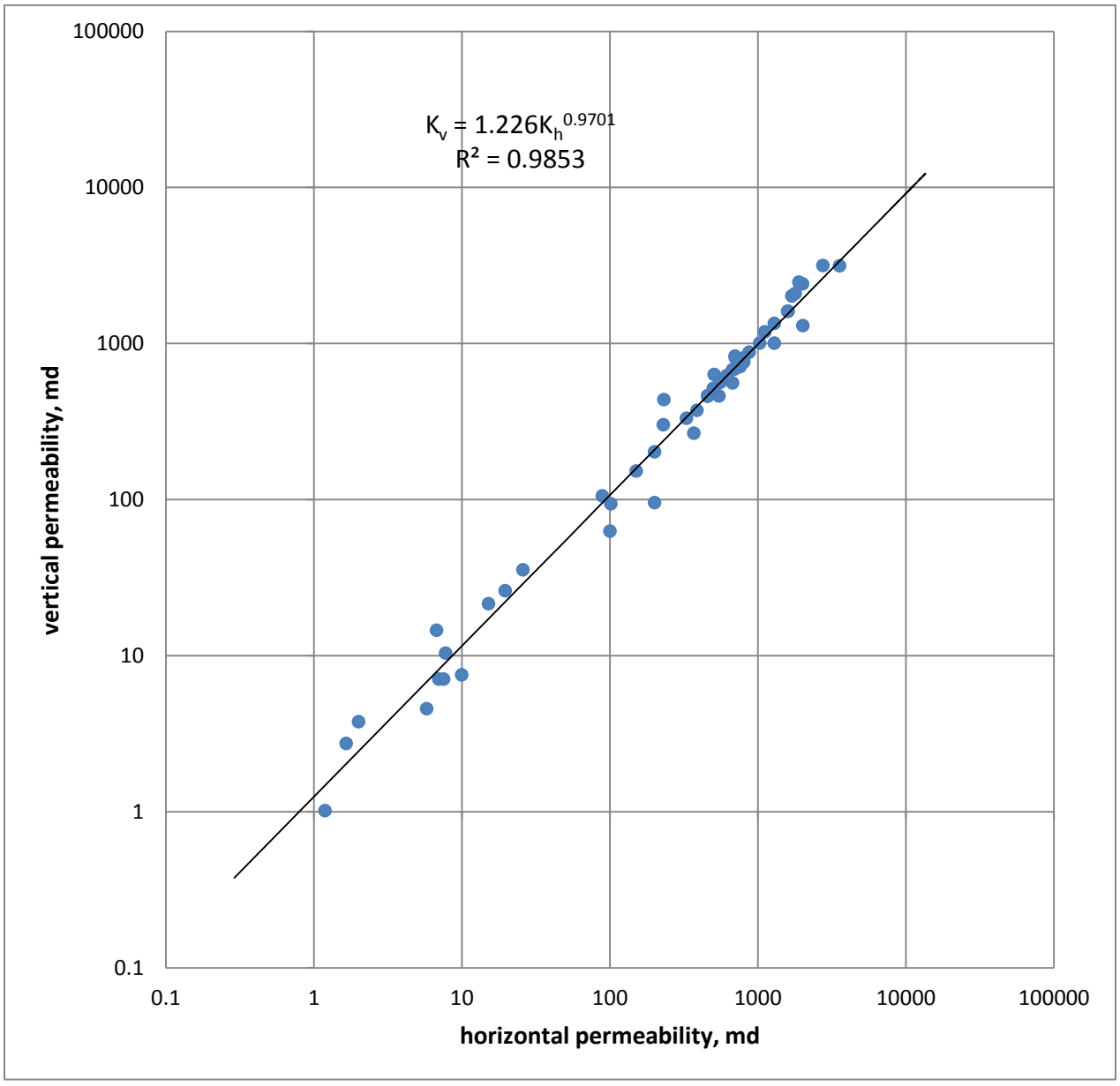

Figure 5.16- Variation of vertical permeability with horizontal permeability for the DRT of the Iranian carbonate case.

The range of the permeability anisotropic ratio, i.e. k_v/k_h, is 0.475 to 2.154 and is shown in figure 5.17.

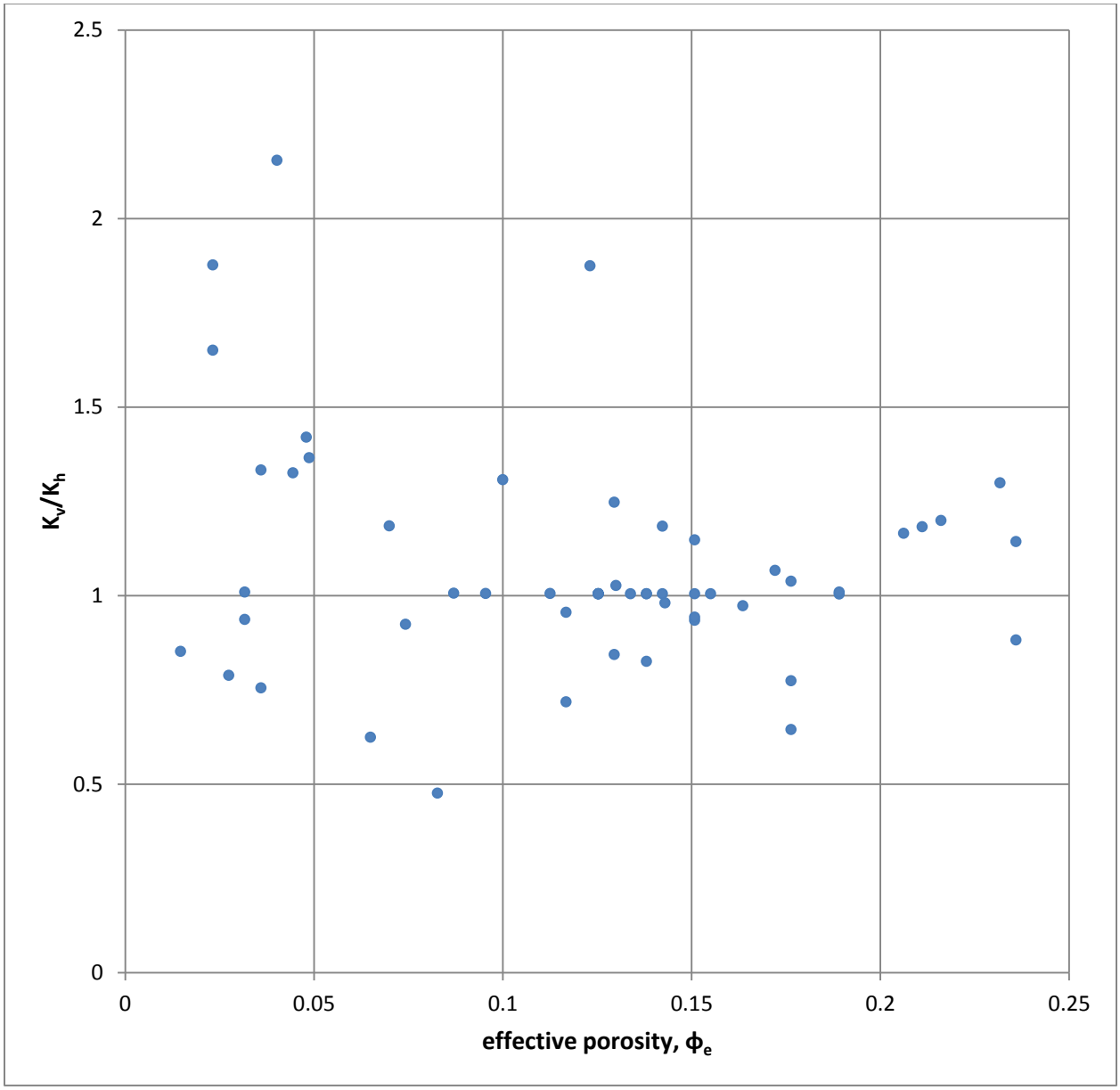

Figure 5.17- Variation of anisotropic permeability ratio with effective porosity for the DRT of the Iranian carbonate case.

The variations of vertical permeability with other parameters are shown in figure 5.18 through 5.20.

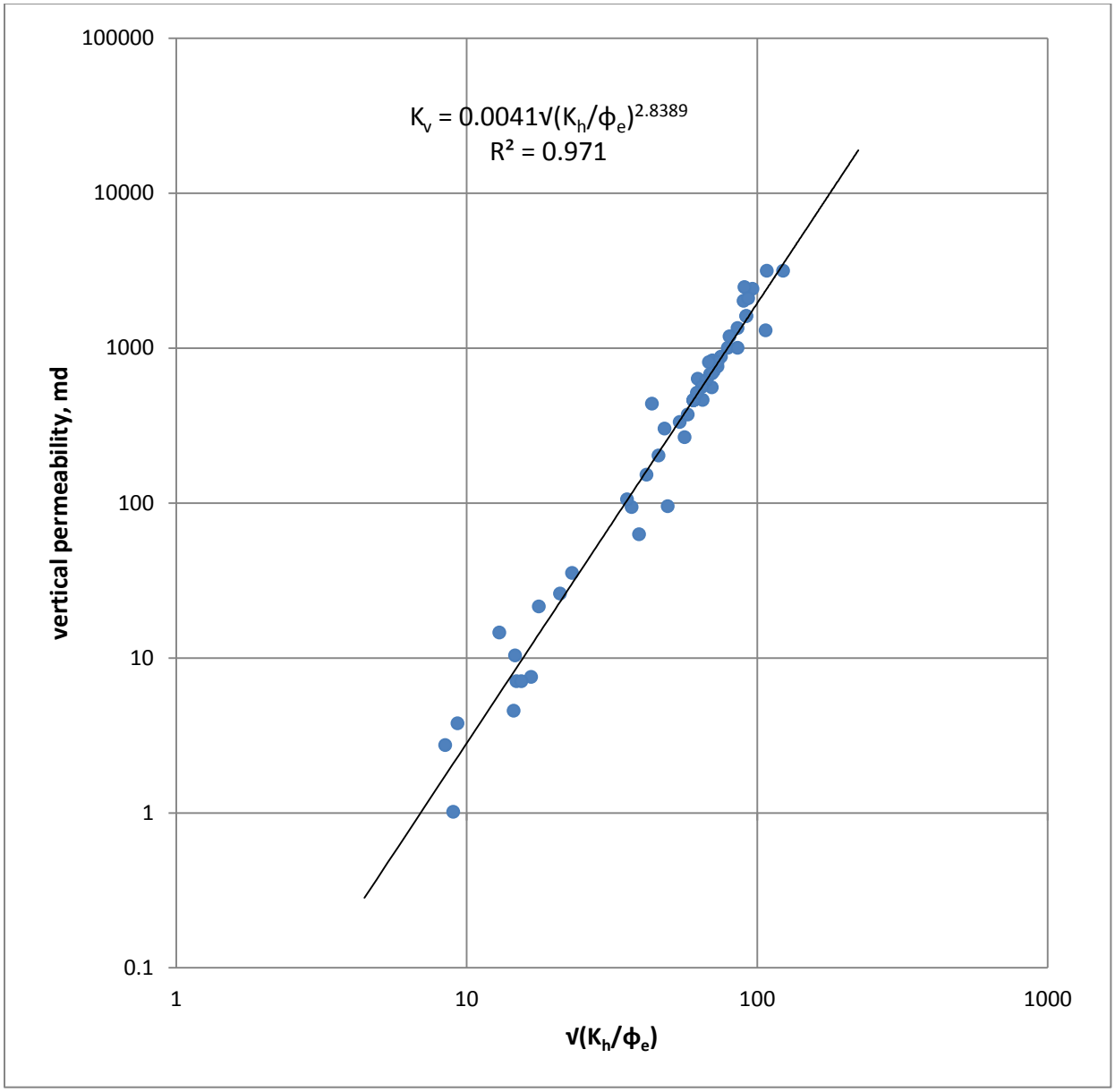

Figure 5.18- Variation of vertical permeability with mean hydraulic radius for the DRT of the Iranian carbonate case.

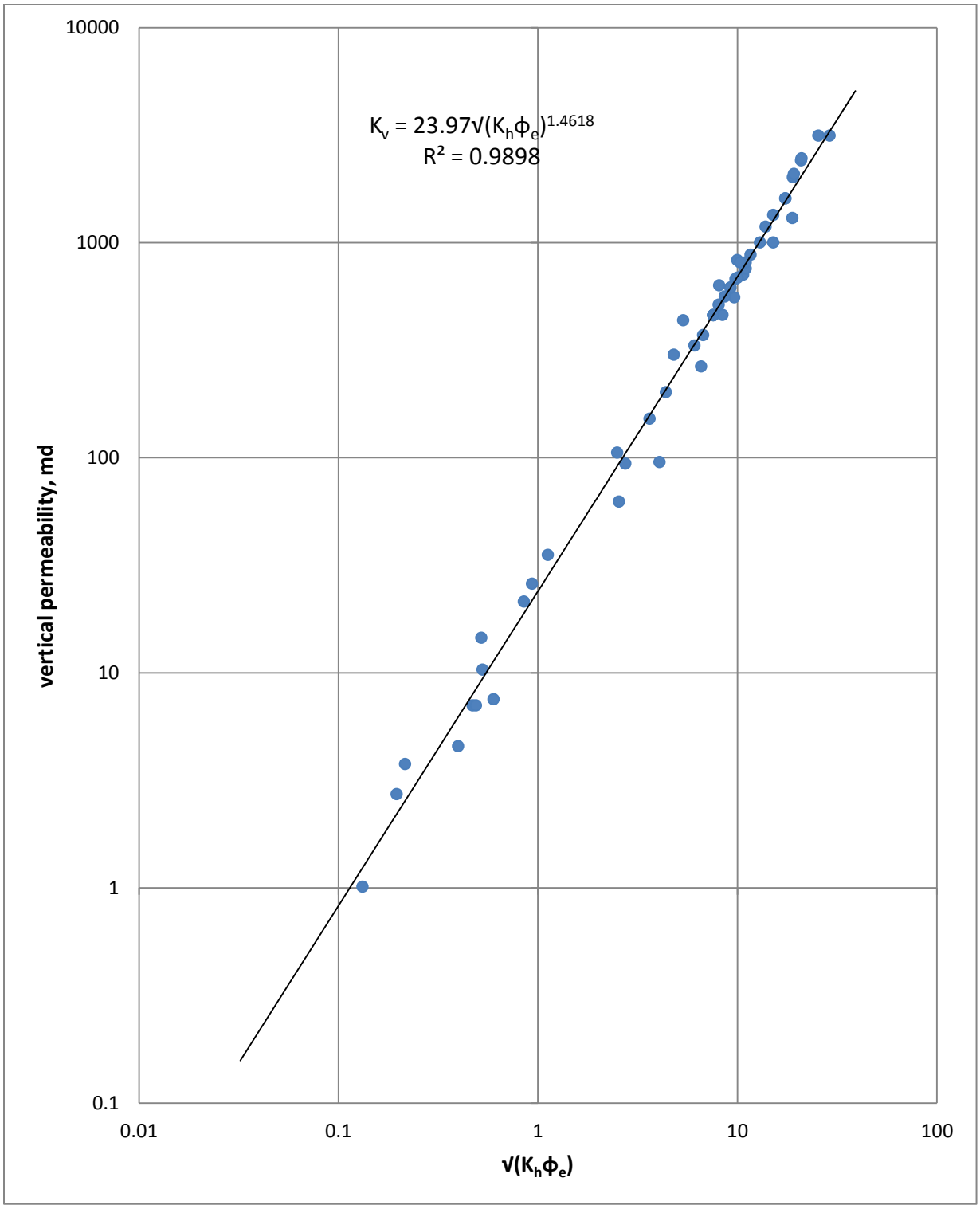

Figure 5.19- Variation of vertical permeability with $\sqrt{K_h \phi_e}$ for the DRT of the Iranian carbonate case.

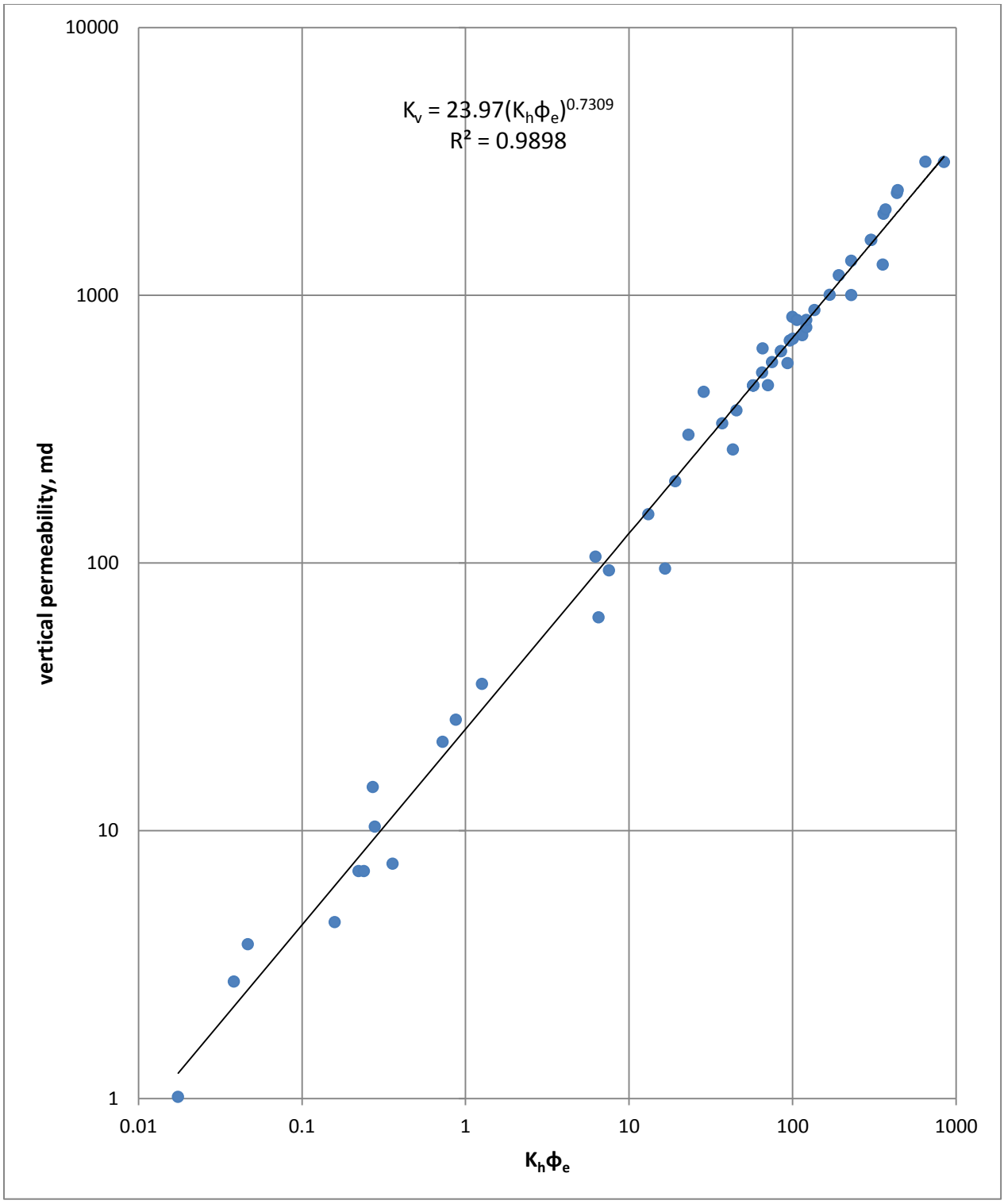

Figure 5.20- Variation of vertical permeability with $K_h\phi_e$ for the DRT of the Iranian carbonate case.

From Figure 5.18 through 5.20, the following correlations are obtained:

$$k_v = 0.0041\left(\sqrt{\frac{k_h}{\phi_e}}\right)^{2.8389} \quad (R^2 = 0.971) \quad \text{..... (5.17)}$$

$$k_v = 23.97\left(\sqrt{k_h\phi_e}\right)^{1.4618} \quad (R^2 = 0.9898) \quad \text{..... (5.18)}$$

$$k_v = 23.97(k_h\phi_e)^{0.7309} \quad (R^2 = 0.9898) \quad \text{..... (5.19)}$$

5.2.2 The Saudi Arabian Carbonate Case

The layer chosen for this analysis is made up of dolomite and this was determined from the wireline-log and core data. The depth of this layer ranges from 3000 ft. to 3050 ft. The average grain density for this layer is 2.88 g/cm^3. The variation of permeability with depth, porosity and grain density is shown in Figures 5.21 through 5.23.

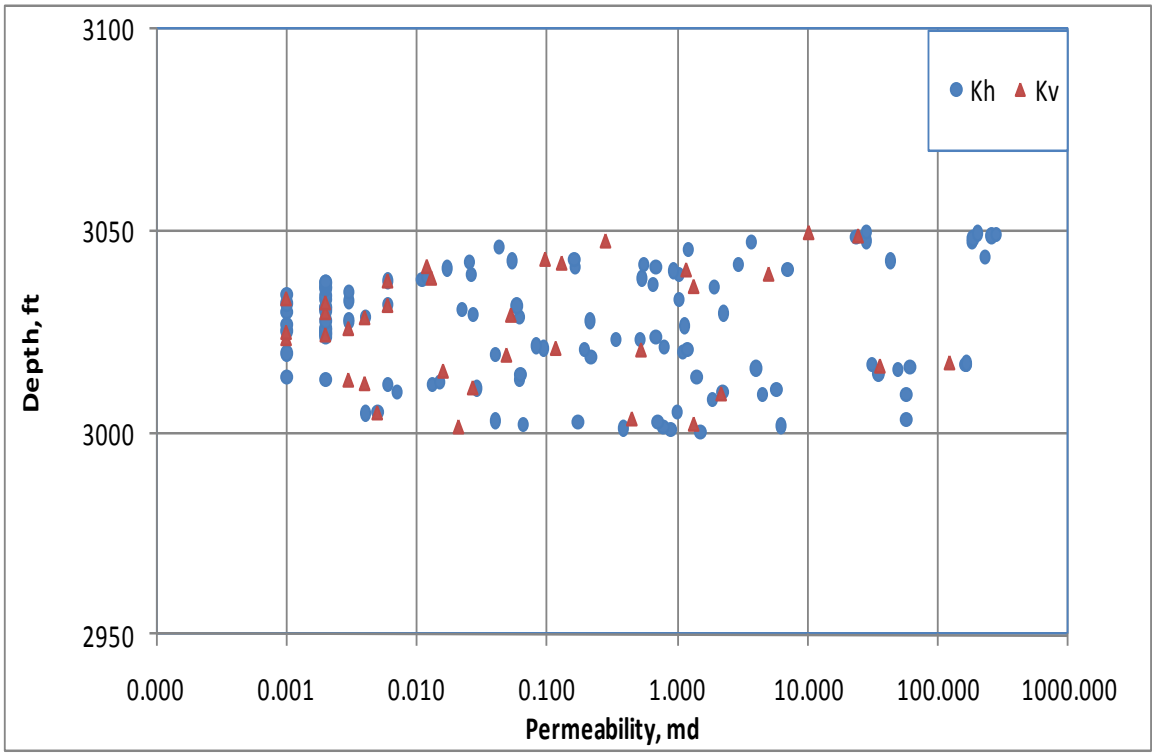

Figure 5.21 - Variation of permeability with depth for the Saudi Arabian carbonate case

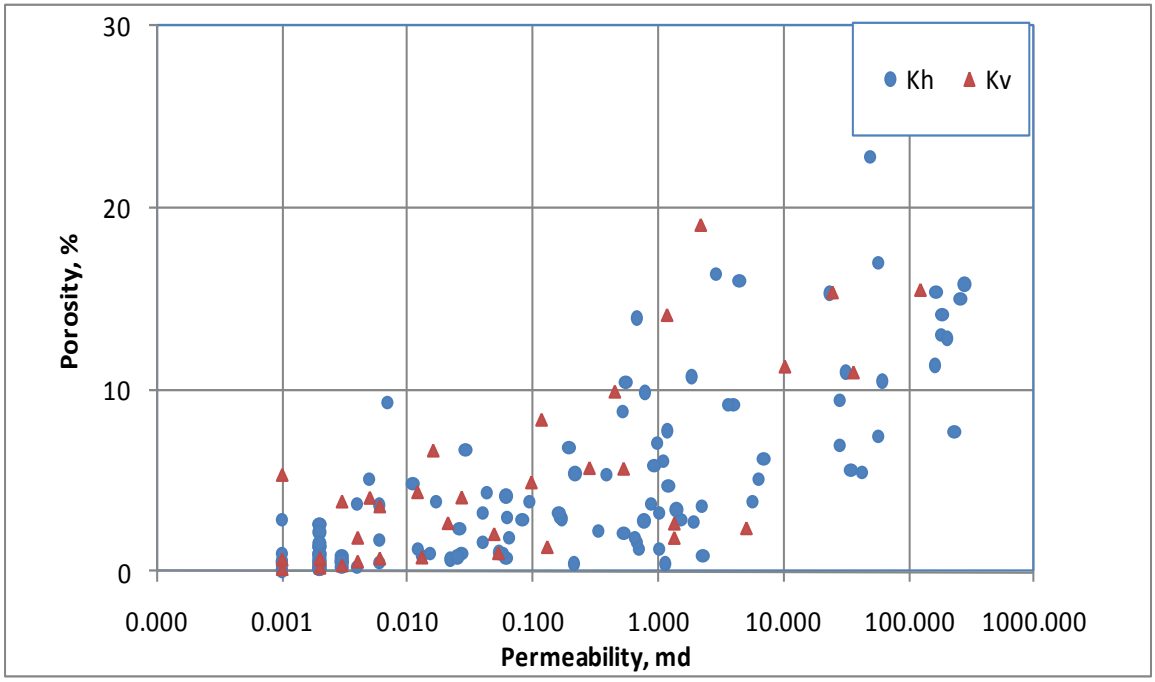

Figure 5.22 - Variation of permeability with porosity for the Saudi Arabian carbonate case

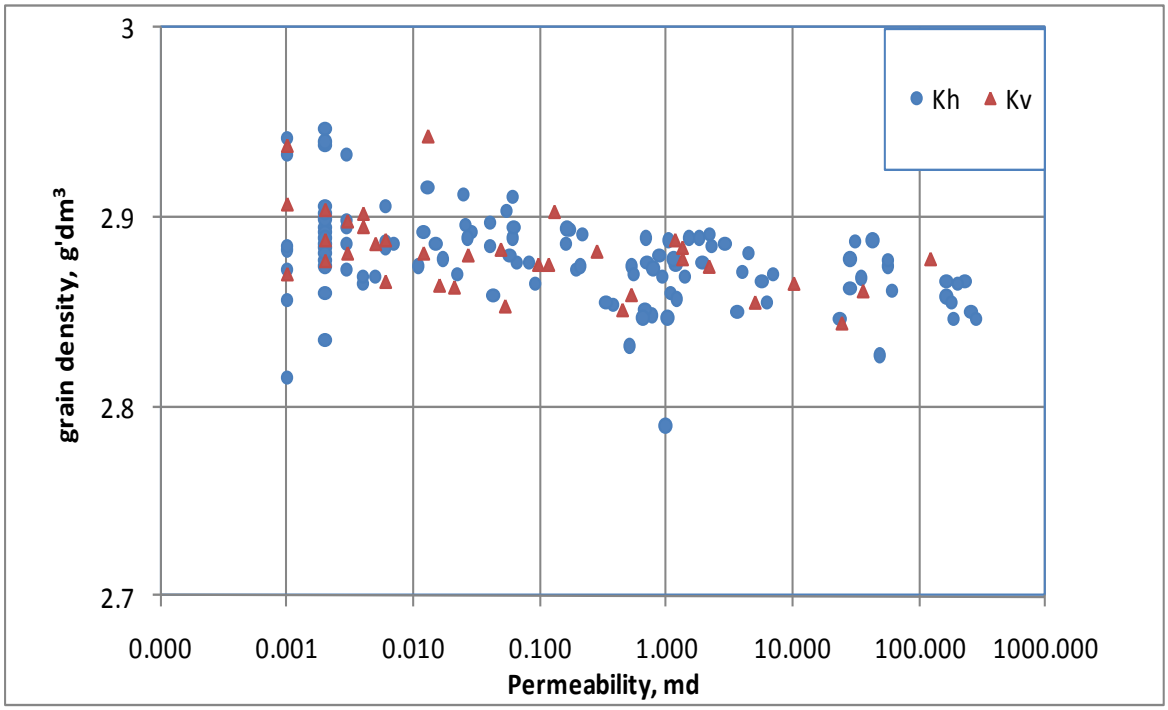

Figure 5.23 - Variation of permeability with grain density for the Saudi Arabian carbonate case

The following equations are obtained from porosity versus permeability plot, since it has the best regression value.

$$\phi = 0.962 \ln(k_h) + 6.4412 \quad \text{..... (5.20)}$$

$$\phi = 1.1096 \ln(k_v) + 7.9698 \quad \text{..... (5.21)}$$

Solving the above two equations we get the following correlation between the vertical permeability and the horizontal permeability.

$$k_v = 0.2522 k_h^{0.867} \quad \text{..... (5.22)}$$

The range of the permeability anisotropic ratio, i.e. k_v/k_h, is 0.119 to 0.632 and is shown in the figure 5.24. The variation of porosity with the anisotropy permeability ratio is shown in figure 5.25.

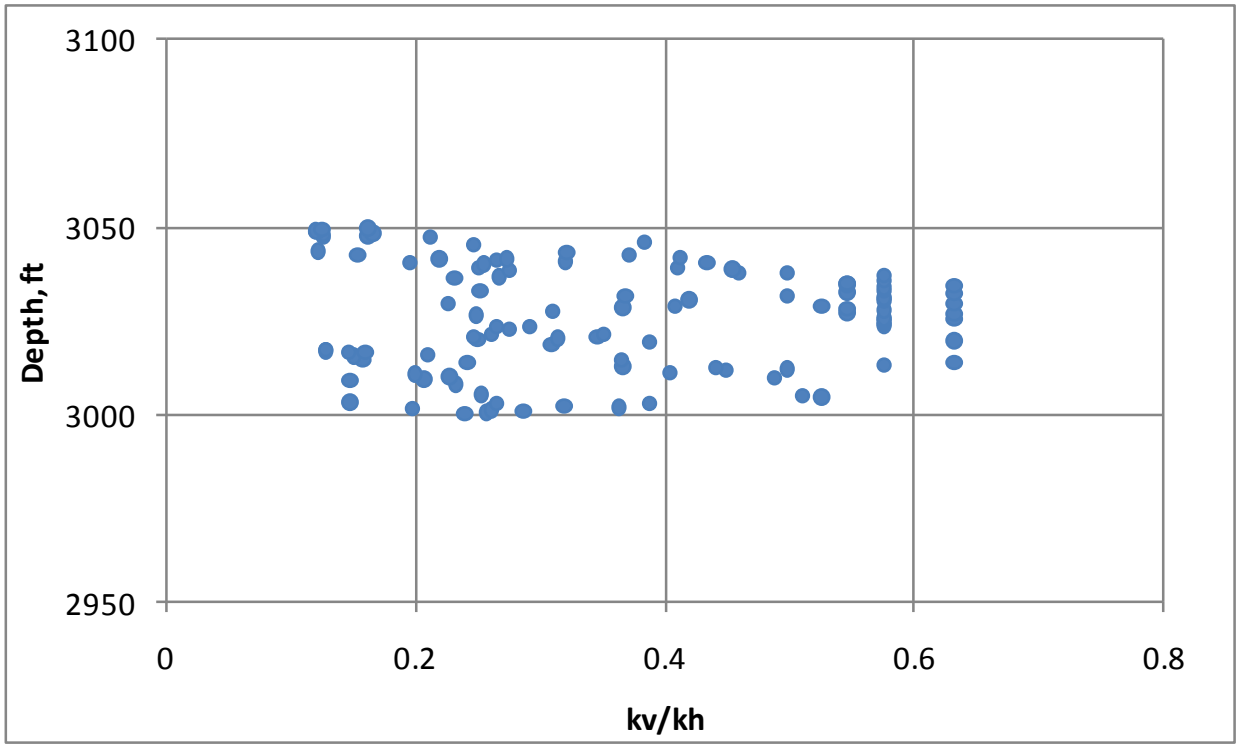

Figure 5.24 - Variation of anisotropic permeability ratio for the Saudi Arabian carbonate case

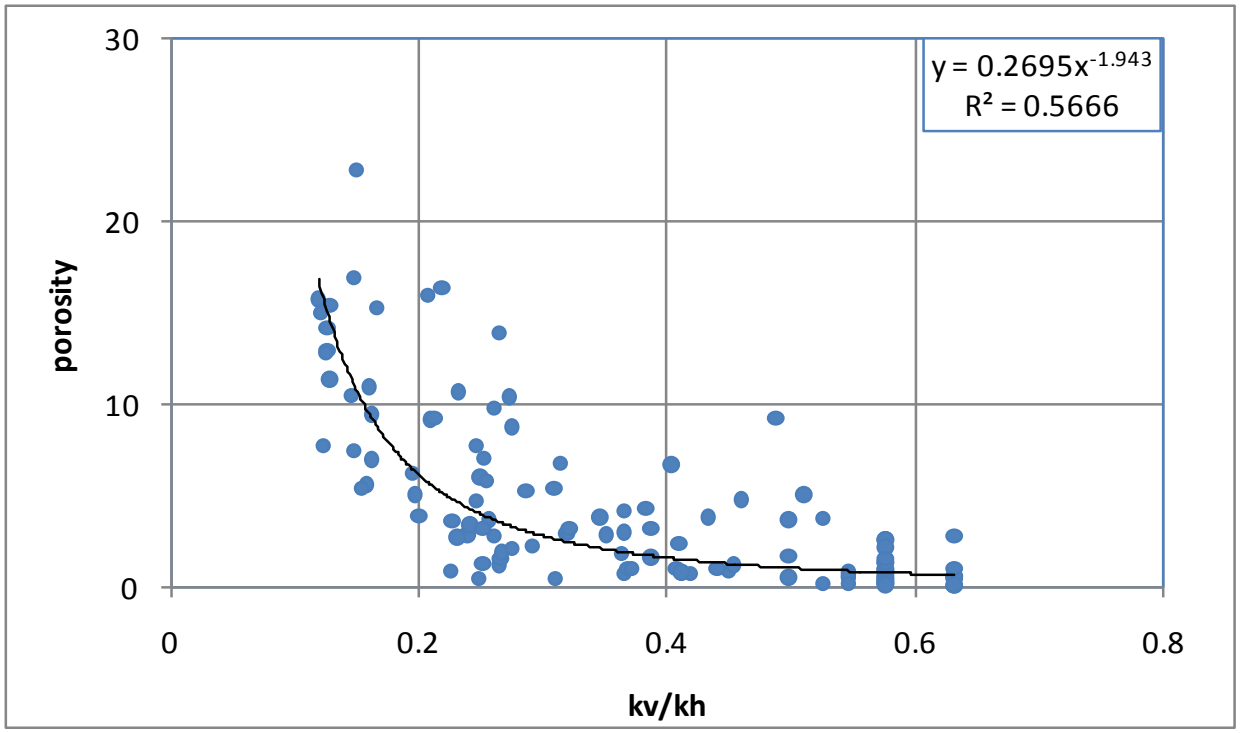

Figure 5.25 - Variation of anisotropic permeability ratio with porosity for the Saudi Arabian carbonate case

From figure 5.23, we get the following correlation:

$$\phi = 0.2695\left(\frac{k_v}{k_h}\right)^{-1.943} \qquad R^2=0.5666 \qquad \text{..... (5.23)}$$

The variation of permeability with other parameters is shown in figures 5.26 through 5.29.

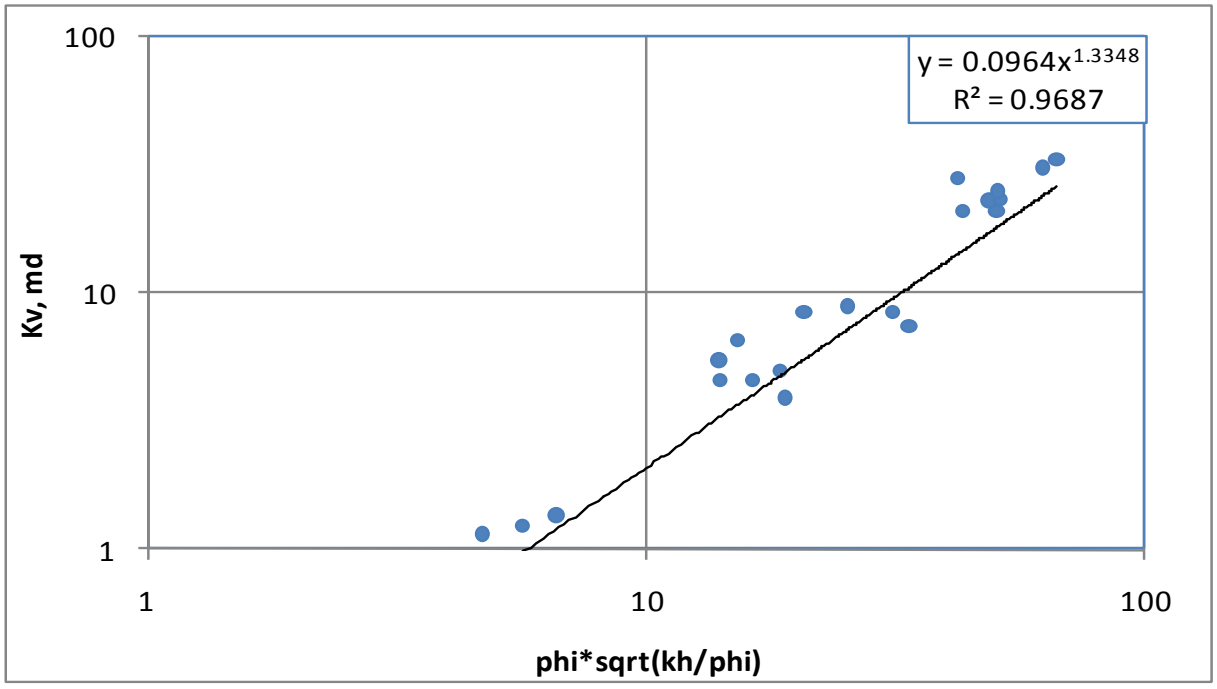

Figure 5.26 - Variation of vertical permeability with $\phi_e\sqrt{\frac{K_h}{\phi_e}}$ for the Saudi Arabian carbonate case.

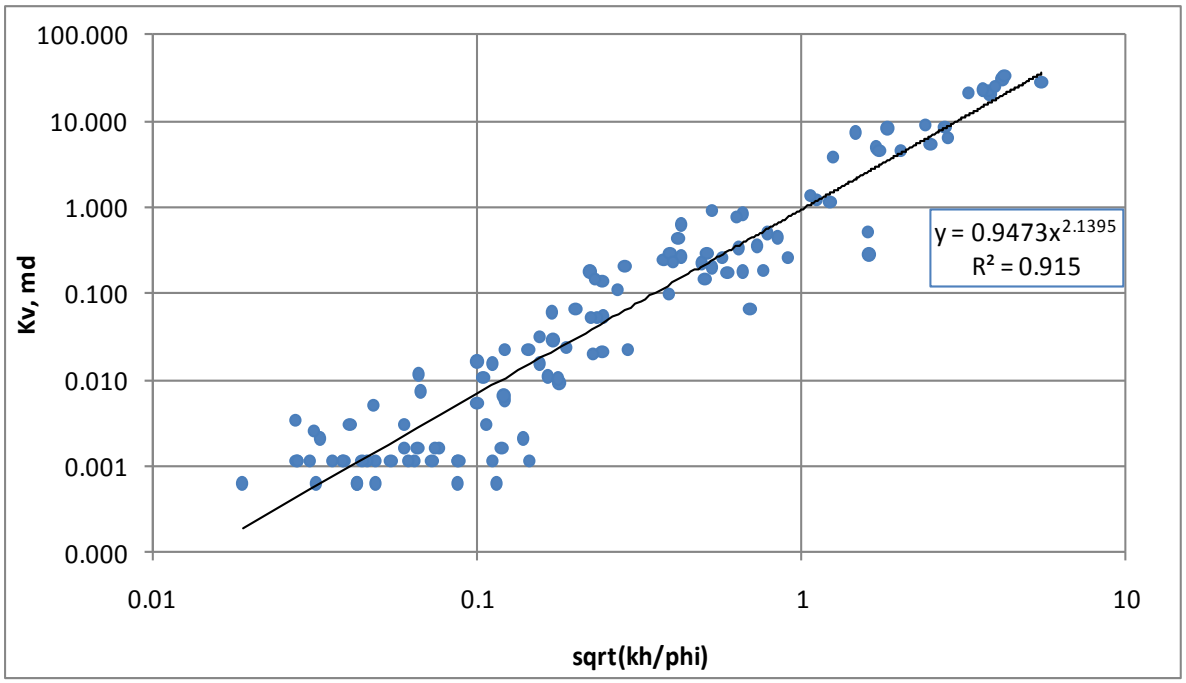

Figure 5.27 - Variation of vertical permeability with $\sqrt{\frac{K_h}{\phi_e}}$ for the Saudi Arabian carbonate case.

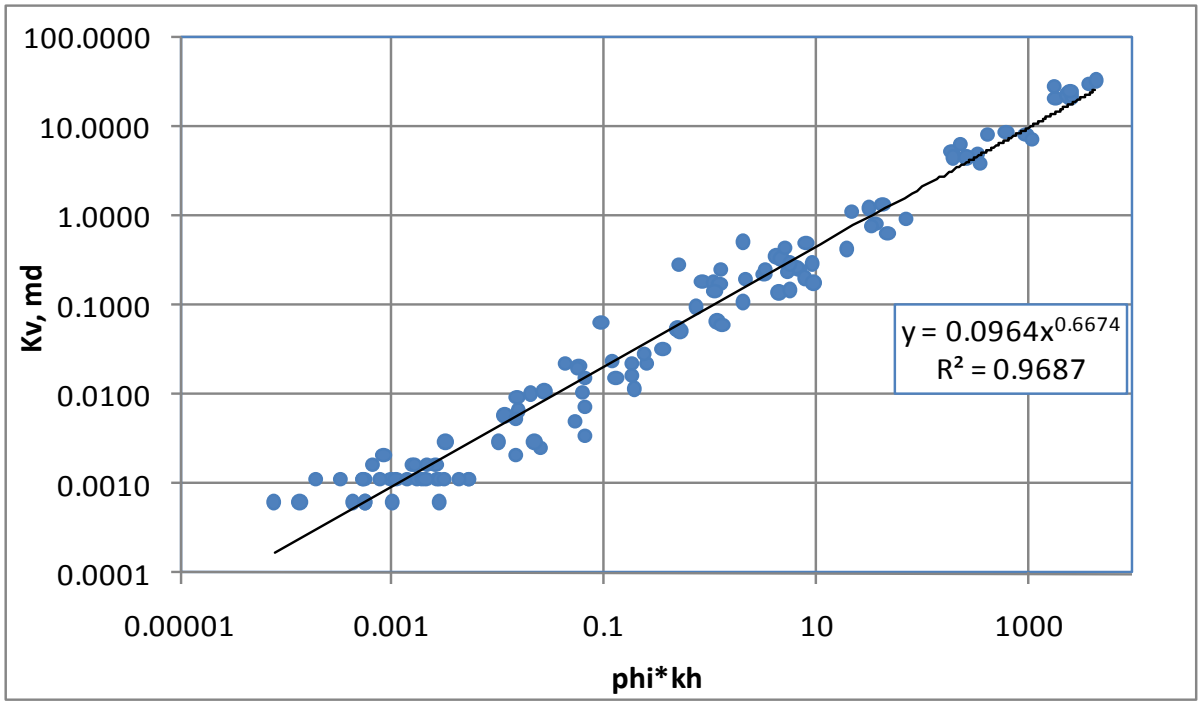

Figure 5.28 - Variation of vertical permeability with $k_h\phi_e$ for the Saudi Arabian carbonate case

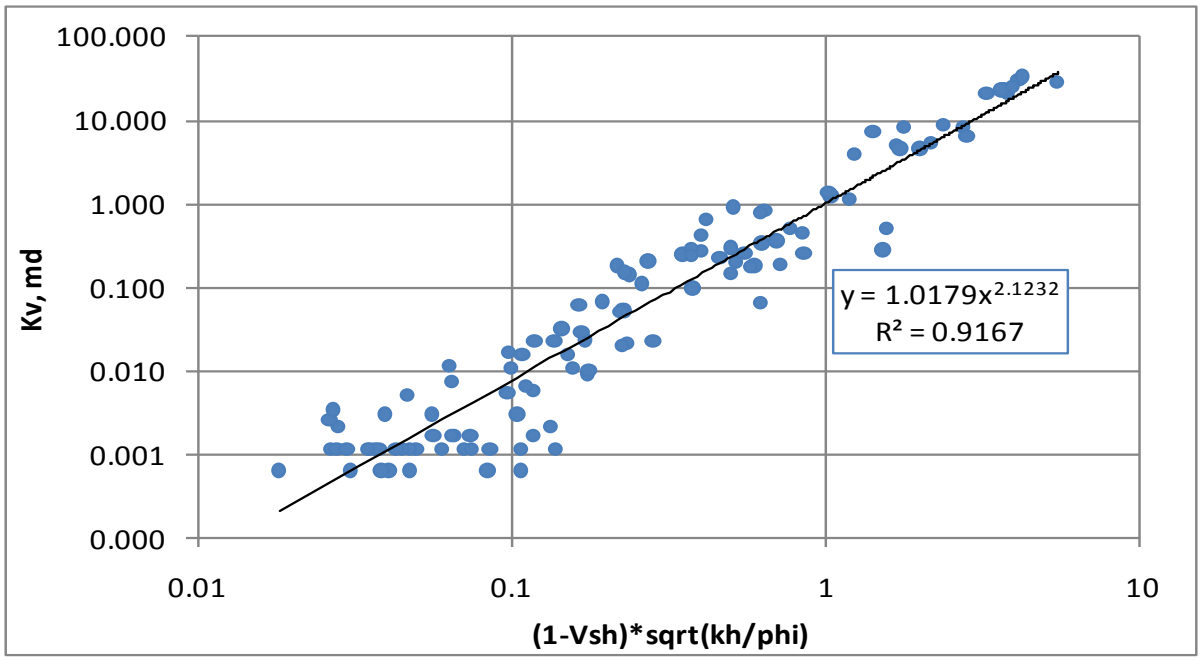

Figure 5.29 - Variation of vertical permeability with $(1 - V_{sh})\sqrt{\frac{K_h}{\phi_e}}$ for the Saudi Arabian carbonate case

From figures 5.26 through 5.29, the following correlations are obtained:

$$k_v = 0.0964\left(\phi_e\sqrt{\frac{k_h}{\phi_e}}\right)^{1.3348} \qquad R^2=0.9687 \qquad \text{..... (5.24)}$$

$$k_v = 0.9473\left(\sqrt{\frac{k_h}{\phi}}\right)^{2.1395} \qquad R^2=0.915 \qquad \text{..... (5.25)}$$

$$k_v = 0.0964(\phi k_h)^{0.6674} \qquad R^2=0.9687 \qquad \text{..... (5.26)}$$

$$k_v = 1.0179\left[(1-V_{sh})\sqrt{\frac{k_h}{\phi}}\right]^{2.1232} \qquad R^2=0.9167 \qquad \text{..... (5.27)}$$

The effective stress is found out from the following equation:

$$\sigma_e = 0.572D \qquad \text{..... (5.28)}$$

The value of pore compressibility c_p is calculated using the following formula:

$$\bar{c}_p = \frac{c_o}{\alpha\Delta\sigma}(1 - e^{-\alpha\Delta\sigma}) \quad \text{..... (5.29)}$$

Matrix compressibility is found out from the following relationship

$$c_r = \phi c_P \quad \text{..... (5.30)}$$

The bulk modulus is the reciprocal of the matrix compressibility, i.e.

$$K = \frac{1}{c_r} \quad \text{..... (5.31)}$$

Since Poisson's ratio of 0.25 holds good for most of the formation, this value is used to find out the Young's Modulus from the following equation.

$$E = 3K(1 - 2\nu) \quad \text{..... (5.32)}$$

The variation of vertical permeability with Young's Modulus is shown in the figure 5.29.

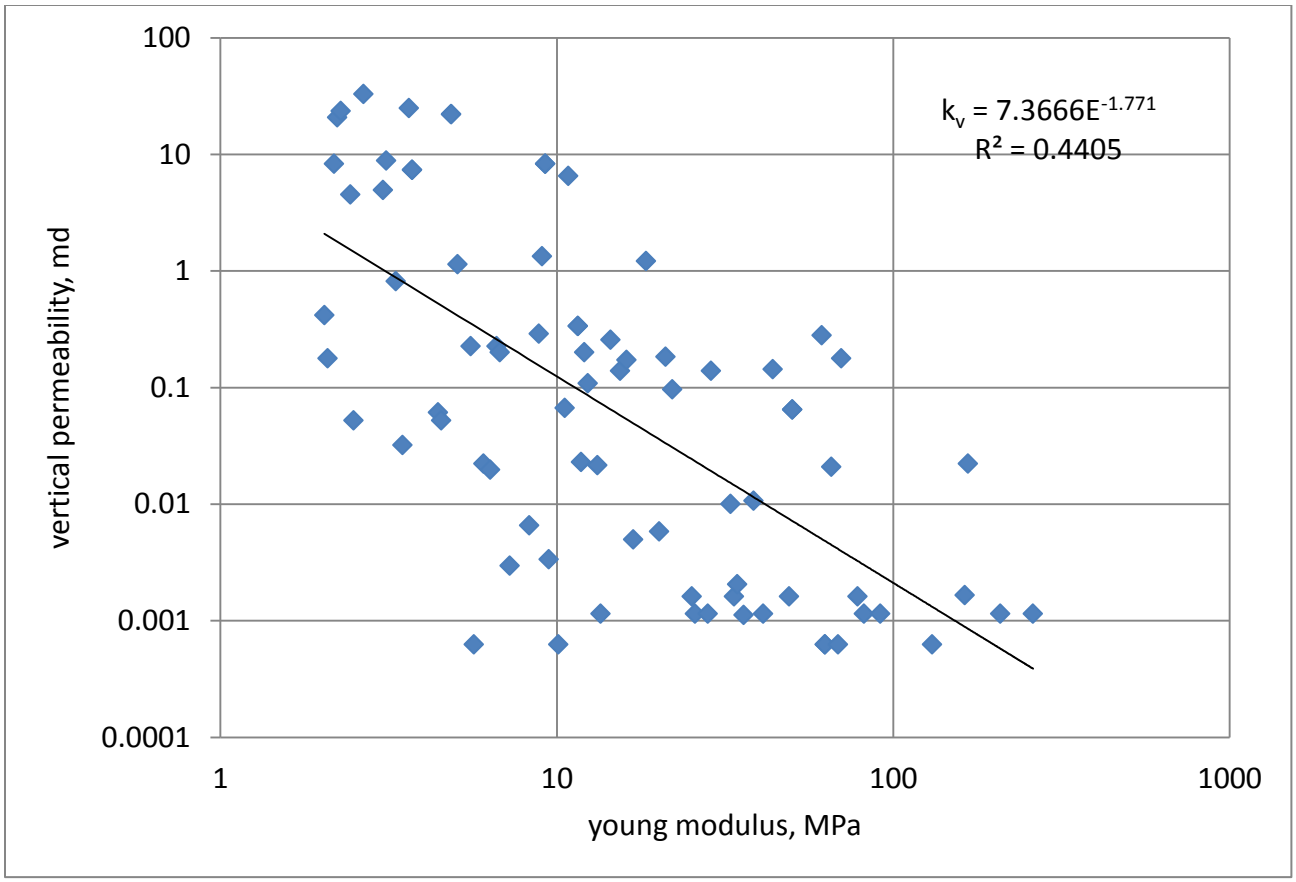

Figure 5.30 - Variation of vertical permeability with Young's modulus for the Saudi Arabian carbonate case

From the figure 5.30, the following correlation can be obtained.

$k_v = 7.3666E^{-1.771}$ R^2=0.4405 ..... (5.33)

From Eq. 5.32 and 5.33, vertical permeability can be correlated to the bulk modulus as follows:

$$k_v = \frac{1.053}{[K(1-2\nu)]^{1.771}} \quad \text{..... (5.34)}$$

CHAPTER SIX

CONCLUSIONS AND RECOMMENDATION

6.1 Conclusions

The conclusions of this work are summarized as follows:

- Core and log data were gathered and used for the analysis of vertical permeability for three fields representing the sandstone, limestone and dolomite reservoir cases.
- The Saudi Arabian carbonate cases were considered for stress sensitivity.
- The permeability anisotropic ratio varies over a wide range for the three reservoir cases.
- Vertical permeability can be estimated from measured horizontal permeability and other petrophysical parameters.
- The vertical permeability relationship that gave the highest correlation coefficient is for the case when the reservoir is divided into discrete rock type.
- Plot of k_v vs. $\sqrt{\frac{k_h}{\phi_e}}$ gave a better correlation coefficient than that of k_v vs. $\left(\phi_e\sqrt{\frac{k_h}{\phi_e}}\right)$ for the sandstone reservoir case.
- Plot of k_v vs $\left(\phi_e\sqrt{\frac{k_h}{\phi_e}}\right)$ gave a better correlation coefficient than that of k_v vs $\sqrt{\frac{k_h}{\phi_e}}$ for the carbonate reservoir cases.
- New vertical permeability correlations for shaly formation were developed.

- Plot of k_v vs $\sqrt{(1-V_{sh})\frac{k_h}{\phi_e}}$ gave a better correlation coefficient than that of k_v vs $(1-V_{sh})\sqrt{\frac{k_h}{\phi_e}}$ for the sandstone reservoir case.
- Due to data limitations, the new correlations were not investigated for the carbonate reservoir cases.

The significances of this study are:

- It incorporates stress effects on reservoirs for better simulation result.
- It gave a better representation of fluid flow behavior for improved reservoir modeling and simulation.
- It helps in choosing proper well spacing and orientation thereby reducing cost of reservoir development especially in offshore locations.
- It helps in the study of the reservoir for remedial works.

6.2 Recommendations

The recommendations bases on the findings in this work are as follows:

- Vertical permeability relationships should be developed for each discrete rock types (DRT) when possible to achieve a much higher correlation coefficient.
- Future work should be done to see which relationship gives the best correlation for sandstone reservoir cases.
- Future work should be done on the new vertical permeability correlations for carbonate reservoir cases.

NOMENCLATURE

A, B = *correlation coefficients*

c = *compressibility, psi^{-1}*

D = *depth, ft.*

E = *Elastic modulus, GPa*

f = *fraction*

F, f = *pore shape factor, dimensionless*

GR = *gamma ray, API*

I = *shale index, dimensionless*

K, k = *permeability, mD*

K = *bulk modulus, GPa*

M = *constrained axial modulus, GPa*

p = *pressure, psi*

V = *volume, fraction*

Greek Letters

α = *pore compressibility constant, psi^{-1}*

β = *strain constant, dimensionless*

ε = *strain, dimensionless*

N = *Poisson ratio, dimensionless*

γ = *grain compressibility, psi^{-1}*

σ = *stress, psi*

δ = *ratio of compressibility of rock matrix to that of bulk, dimensionless*

ε_l, β = *parameters of Langmuir curve match to volumetric strain change because of matrix shrinkage (ε_l is dimensionless and β is in psi^{-1})*

ϕ = *porosity, dimensionless*

Subscripts

CS = *clean shale*

h = *horizontal direction*

i = *initial state*

m = *rock matrix*

o = *initial conditions*

p = *pore*

ps = *pore shape*

sh = *shale*

v = *vertical direction*

REFERENCES

1. Ahr, W.M. 2007. Geology of Carbonate Reservoirs: The Identification, Description, and Characterization of Hydrocarbon Reservoirs in Carbonate Rocks. Wiley-Interscience.
2. Ayan, C., Colley, N., Goode, P., Halford, F., Joseph, J., Mongini, A., Pop, J., 1994. Measuring Permeability Anisotropy: The Latest Approach. *Oilfield Review* **6** (4): 24-35.
3. Carman, P. C., 1939. "Permeability of Saturated Sands, Soils and Clays." *J. Agr. Sci.*, Vol. 29, Also, *J. Soc. Chem. Ind.*, pp. 57–58.
4. Celis, V., Silva, R., Ramones, M., Guerra, J., Da Prat, G., 1994. A new model for Pressure Transient Analysis in stress sensitive Naturally Fractured Reservoirs SPE 23668.
5. Dobrynin, V.M., 1962. Effect of Overburden Pressure on Some Properties of Sandstones. *SPE J* **2** (4): 309-330.
6. Economides, M. J., Buchsteiner, H., Warpinski, N. R., 1994. Step-pressure test for stress sensitive permeability determination. SPE 27380.
7. Kasap, E., 2001. Estimating kv/kh Ratio for Conductive and Nonconductive Shales and Mudstones. SPE-68782.
8. Kozeny, J., 1927. "Über kapillare Leitung des Wassers im Boden (Aufstieg Versikerung und Anwendung auf die Bemasserung)." Sitzungsber Akad., Wiss, Wein, Math- Naturwiss, KL, Vol. 136 (Ila), pp. 271–306.
9. Lorenz, J.C., 1999. Stress-sensitive Reservoirs, *J Pet Tech* **51** (1): 61-63. SPE-50977-MS.
10. McKee, C.R, Bumb, A.C., and Koenig, R.A. 1988. Stress-Dependent Permeability and Porosity of Coal and Other Geologic Formations. *SPE Form Eval* 3 (1): 81-91. SPE-12858-PA.
11. Palmer, I. and Mansoori, J. 1998. How Permeability Depends on Stress and Pore Pressure in

Coalbeds: A New Model. *SPE Res Eval & Eng* **2** (6): 539-544. SPE-52607-PA.

12. Pedrosa, O. A., 1986. Pressure transient response in stress sensitive formations. Presented at the SPE regional meeting, Oakland. SPE 15115.
13. Qun, L., Wei, X., Yuan, J., Cui, Y., and Wu, Y. 2008. Analysis of Stress Sensitivity and its Influence on Oil Production from Tight Reservoirs. SPE 111148-MS.
14. Ruan, M. and Wang, L. 2002. Low-permeability Oilfield Development and Pressure-sensitivity Effect. *Acta Petrolei Sinica* **23** (2): 73-76.
15. Samaniego, F., Cinco-Ley, H. 1989. On the dependent of the pressure dependent characteristics of a reservoir through transient pressure testing. 64th ATCE of SPE San Antonio Texas Oct. 8-11, SPE 19774.
16. Tiab, D. and Donaldson, E. 2004. *Petrophysics*, second edition. Oxford: Elsevier.
17. Vairogs, J., Hearn, C.L., Dareing, D.W., and Rhoades, V.W. 1971. Effect of Rock Stress on Gas Production from Low-Permeability Reservoirs. *J Pet Tech* **23** (9): 1161-1167. SPE-3001-PA.
18. Vairogs, J., Rhoades, V.W. 1973. Pressure transient tests in formations having stress sensitive permeability. JPT (Aug.) 965-970.
19. Zahaf, K., Tiab, D. 2002. Vertical Permeability From In Situ Horizontal Measurements in Shaly-Sand Reservoirs, *J Can Pet Tech* **41** (8): 43-50. PETSOC-02-08-01-P.
20. Zheng Z., Khodaverian, M., and McLennan, J.D. Static and Dynamic Testing of Coal Specimens," paper 9120 presented at the 1991 Society of Core Analysts Fifth Annual Technical Conference, August.